# Chalk: composition, diagenesis and physical properties

IDA L. FABRICIUS

Fabricius, I. L. 2007–03–12: Chalk: composition, diagenesis and physical properties. *Bulletin of the Geological Society of Denmark*, Vol. 55, pp. 97–128. © 2007 by Geological Society of Denmark. ISSN 0011–6297.

File replaced 2020–07–21: Erroneous formulas 8, 9 and 11 in the original publication are corrected.

File replaced 2026–02–23: Erroneous formula 11 in the 2020-07-21 version is corrected.

Chalk is a sedimentary rock of unusually high homogeneity on the scale where physical properties are measured, but the properties fall in wide ranges. Chalk may thus be seen as the ideal starting point for a physical understanding of rocks in general. Properties as porosity, permeability, capillary entry pressure, and elastic moduli are consequences of primary sediment composition and of subsequent diagenetic history as caused by microbial action, burial stress, temperature, and pore pressure. Porosity is a main determining factor for other properties. For a given porosity, the specific surface of the sediment controls permeability and capillary entry pressure. As diagenesis progresses, the specific surface is less and less due to the calcite component and more and more due to the fine-grained silicates, as a reflection of the coarsening and cementation of the calcite crystals. The elastic moduli, which define sonic velocity, are for a given porosity mainly controlled be the degree of pore-stiffening cementation, which may be quantified by effective medium modeling.

Diagenetic processes include mechanical compaction, pore-stiffening cementation, dissolution, and pore-filling cementation. Processes involving clay, silica, and calcite are interlinked, but progress differently in different localities. This partly depends on primary sediment composition, including organic content, which may induce the formation of concretions by microbial action. The diagenetic processes also depend on water depth, rate of burial, and over-pressuring. These factors cause the stress, temperature and pore-pressure to increase at different rates during burial in different localities.

*Key: words:* Chalk, diagenesis, physical properties, elasticity, porosity, permeability, capillary entry pressure.

*Ida L. Fabricius* [*ilf@er.dtu.dk*], *Technical University of Denmark, Institute of Environment and Resources, Bygningstorvet 115, DTU, DK-2800 Kgs. Lyngby, Denmark.*

Chalk is of wide technical interest. It is used as a raw material for cement, as a means of controlling acidity in soil and neutralizing acid gasses generated in power plants, as filler in paper and plastic and as white pigment. Major structures as the Channel Tunnel and the Øresund Fixed Link involved construction on chalk and tunneling in chalk. Where chalk has low porosity it may even be used as a building stone. Where more porous, chalk may be an important aquifer as in Southern England and Eastern Denmark, and last but not least it forms the reservoir for petroleum in the central North Sea. It is thus not solely of geological interest to understand the physical properties of chalk and to find out how geological processes control these physical properties. In the present paper chalk is discussed from the viewpoint of the technical geologist and main emphasis will be given to work completed by the author and her collaborators.

Chalk is a sedimentary rock where diagenetically altered calcareous nannofossils constitute a main component. It is typically derived from calcareous ooze of the ocean where temperature and nutrient conditions of the surface waters favor calcareous plankton (Berger & Winterer 1974). Where surface water is cold, siliceous ooze rather than calcareous ooze is found, and near the shore calcareous macrofossils or siliciclastic deposition dominate. The depth to which chalk deposition is possible is controlled by the solubility in the ocean water of the dead remains of calcitic plankton, described as the carbonate compensation depth. It has varied through geologic history and varies with latitude and from ocean to ocean but at present ranges around 4.5 km (*e.g.* Berger 1973; Farrell & Prell 1989). The familiar chalk of the North Sea basin is recognized to be the result of a marked transgression in the Cretaceous causing parts of the continental shelf to enjoy sedimentary

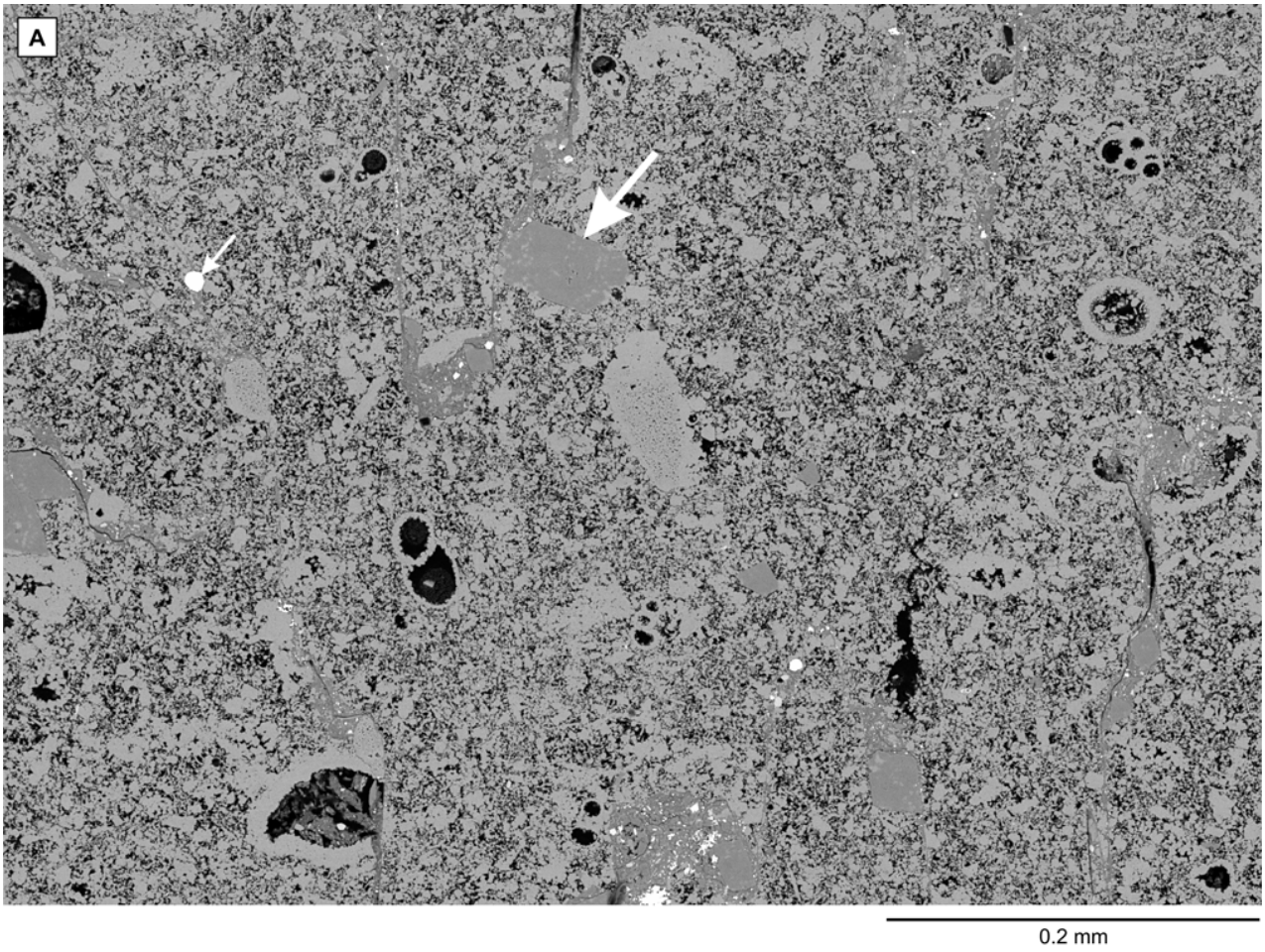


Fig. 1. Backscatter electron micrograph of a stylolite from Dan field, well M-2X, 1934 m sub sea, in microfossil bearing mudstone of Maastrichtian age from the Tor Formation. The stylolite is outlined by silicates (grey) and accompanied by euhedral dolomite rhombs (light grey, big arrow) and pyrite (white, small arrow). The outline of the stylolite is sketched in the lower image. Average porosity is 26.5%. Porosity variation is visible from the distribution of the very light grey calcite particles. No preferred lowering of porosity along the stylolite was noted. Intra-fossil as well as inter-particle porosity are seen. Intra-fossil porosity in some of the microfossils is reduced by calcite cement. The observation of dolomite crystals associated with stylolites in North Sea chalk may be a reflection of dissolution of Mg-bearing calcite along the stylolite (Wanless 1979).

environments similar to what we today find at deep sea oceanic plateaus and ridges (Håkansson *et al.* 1974; Surlyk 1997).

As seen from a 100 m distance chalk looks as a homogeneous white sedimentary rock; but the observer facing an outcrop or a drill core may find traces of bioturbation, hardgrounds, and intervals where the presence of clasts of chalk or other rocks in massive chalk indicate sediment transport by mass flow. Intervals may also be found where lamination and sorting indicate sediment transport by turbidites or traction currents or winnowing (Bromley 1967; Hancock 1975; Berger & Johnson 1976; Perch Nielsen 1979; Ekdale & Bromley 1984; Herrington *et al.* 1991; Scholle *et al.* 1998; Damholt & Surlyk 2004). The observer may also find intervals rich in siliceous fossils or clay, or the diagenetic equivalents chert, flaser structures

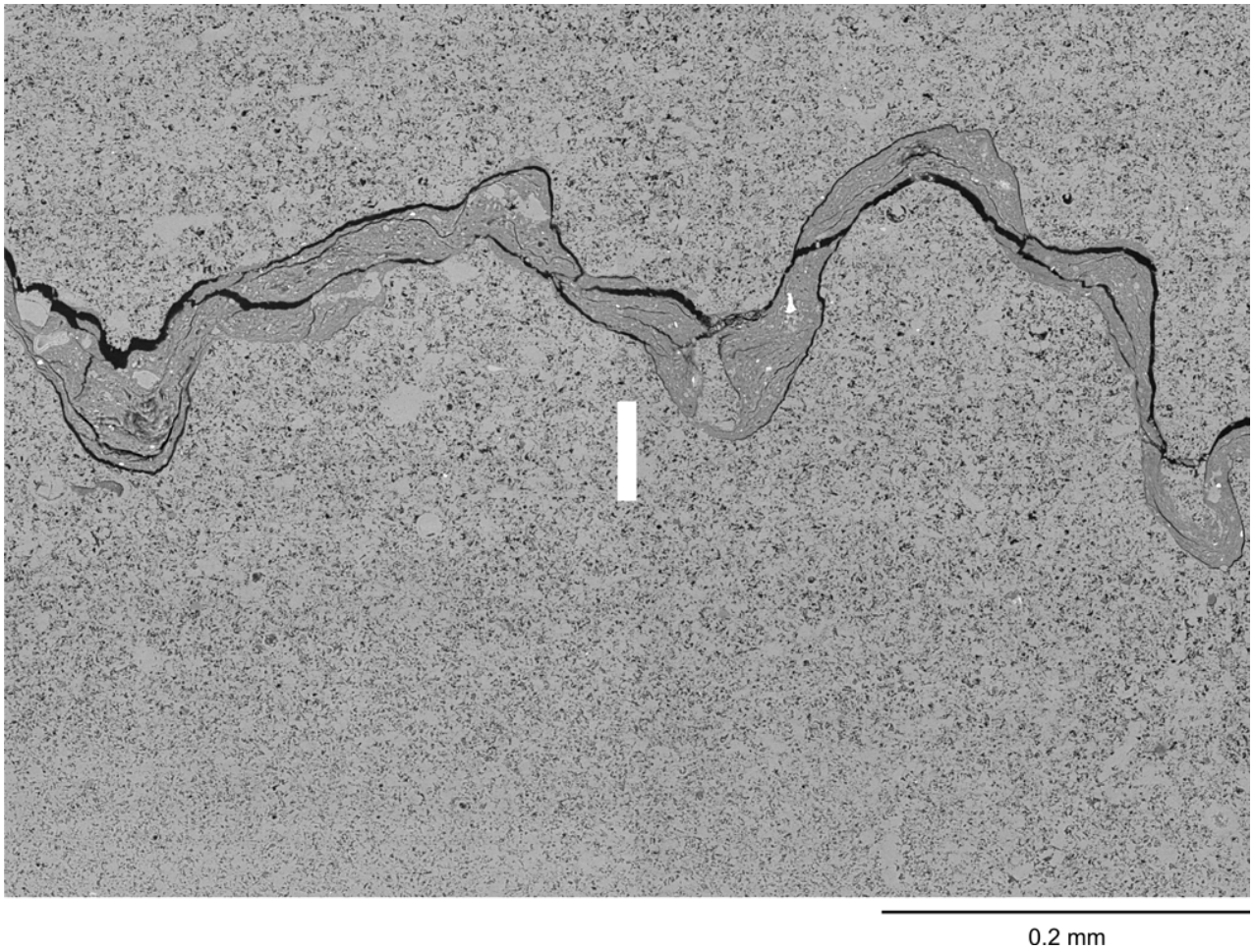


Fig. 2. Backscatter electron micrograph of stylolite from the Ontong Java Plateau, ODP Site 807, 1275.2 m below sea floor, in chalk facies limestone of upper Campanian – lower Maastrichtian age. The clay drape contains quartz and smectite-illite. White clasts in clay drape are probably biogenic apatite. White crystals in limestone are probably authigenic barite. Laboratory bulk sample porosity is 21.9%. Pore-filling calcite cement is localized at bioclasts rather than along the stylolite.

and stylolites (Kennedy & Garrison 1975; Kastner 1981; Hill 1983).

If the observer sampling the chalk prepares thin sections and use an optical microscope or a scanning electron microscope, the chalk appears heterogeneous also at this scale: microfossils, clasts of larger fossils, chalk or other types of rock are unevenly distributed in a matrix of more or less disintegrated and recrystallized nannofossils. The chalk may have signatures of diagenesis: microfossils and fractures may be found to be more or less cemented by calcite, clay or silica. Other diagenetic signatures include molds, frequently after presumably siliceous fossils, pyrite and dolomite crystals as well as stylolites (Fig. 1, 2).

If now the observer takes a small sample and uses the high magnification of a scanning electron microscope it will appear that on this scale some of the homogeneity returns: each chalk particle is an aggregate of crystals or a single crystal of calcite with smooth crystal surfaces (Fig. 3; Andrews *et al.* 1975). If the observer rather uses an atomic force microscope where the resolution is extreme, the smooth calcite crystals will reveal themselves as rugged landscapes where calcium and carbonate ions leave and reunite with the calcite surface and thus persistently change the surface topography (Fig. 4; Stipp 2002).

When studying chalk, the scale chosen must depend on the purpose of study and the scale at which the relevant observations and measurements can be made. When chalk is used as a raw material, or must be excavated, or forms the basis for construction work, or when chalk acts as a reservoir for hydrocarbons or water, the chalk properties are relevant on an outcrop scale: several tens of meters in depth by square-kilometer order of size in the horizontal

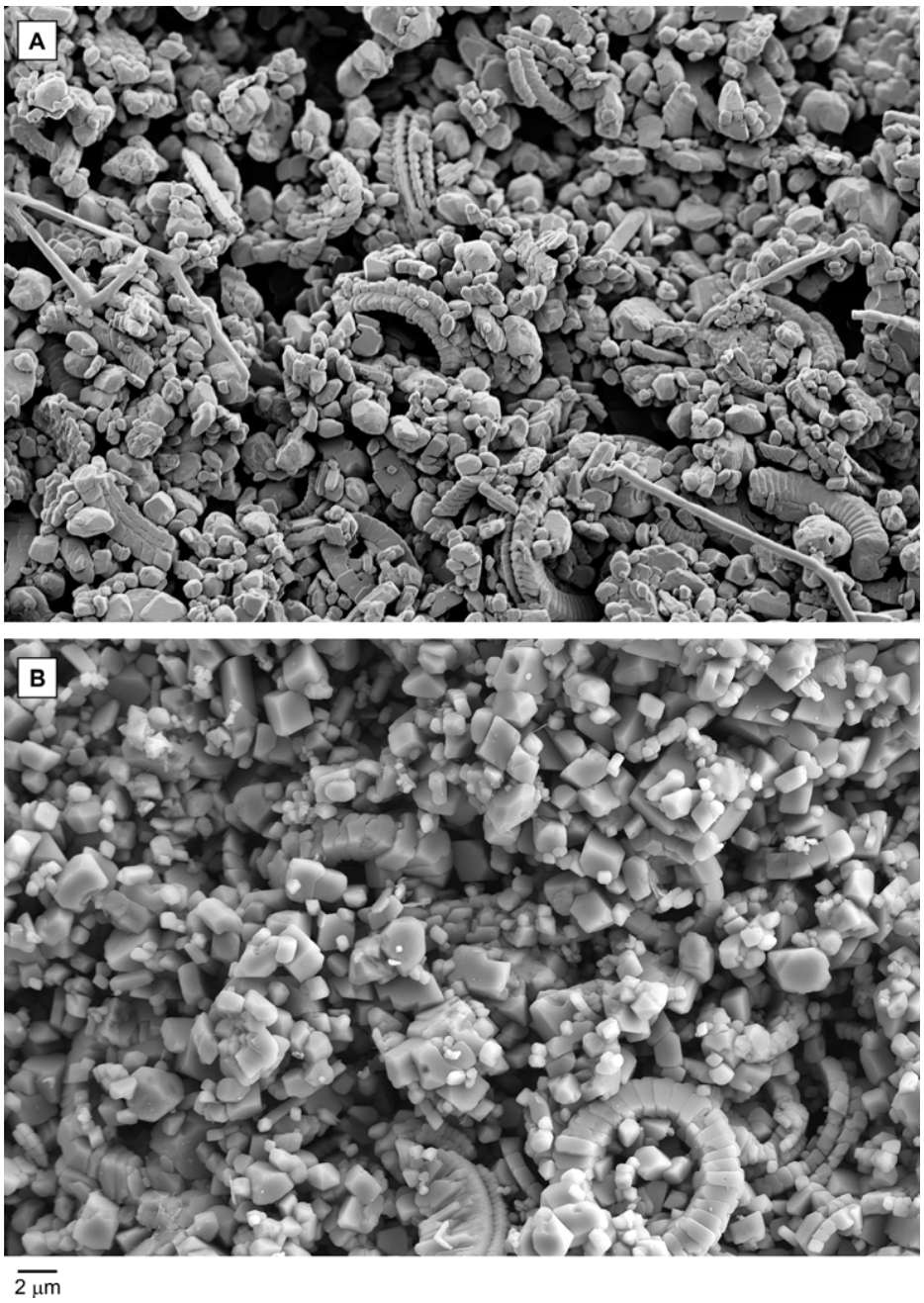


Fig. 3. Scanning electron micrographs of chalk of Maastrichtian age.
(A) Partially or fully broken coccoliths from Stevns chalk with a porosity of 50%. The thin rods are modern organic remains.
(B) Recrystallized chalk from Tor Formation of South Arne field with a porosity of 30%. Images were recorded by Morten Hjuler.

plane. Some physical properties as *e.g.* sonic velocities can be measured on that scale. At that large scale other properties may be derived by sampling and upscaling from a smaller scale (Frykman & Deutsch 2002). For an understanding of how the chalk composition and physical properties interrelate, the scale must be chosen on the cm to dm scale where several measurements and observations can be made: elasticity, strength, porosity, permeability, specific surface, capillary pressure curves, ultrasonic velocity, microtexture, mineralogical and chemical composition, wetting properties, ratio of stable isotopes; and also magnetic susceptibility and electric resistivity. Please note the latter two properties are not discussed here, and not fracturing either, although fracturing may have a large influence on the physical properties of a given chalk unit. The focus is on the chalk material itself.

In this paper emphasis will be given to chalk microtexture and burial diagenesis, on the resulting elastic properties, porosity, permeability and capillary entry pressure and how they vary among some hydrocarbon bearing North Sea chalk fields: Ekofisk, Valhall, South Arne, Valdemar, Tyra, Gorm and Dan

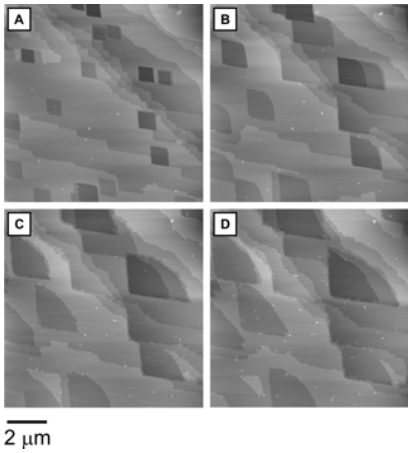


Fig. 4. Atomic force micrographs of calcite surface. In contact with a water phase, calcium and carbonate ions leave and settle on the calcite surface, so that the surface topography smoothens. Net dissolution or net precipitation depends on the relative rate of ions leaving and settling on the surface. Images (A) through (D) demonstrate how etch pits formed by adding milli-Q water to cleaved Iceland spar changes shape during 30 minutes (Harstad & Stipp 2007). Each step on the shown surface ({1 0 î 4}) represents one layer of ions, or ca 3 Å (0.0003 μm, Henriksen *et al.* 2004).

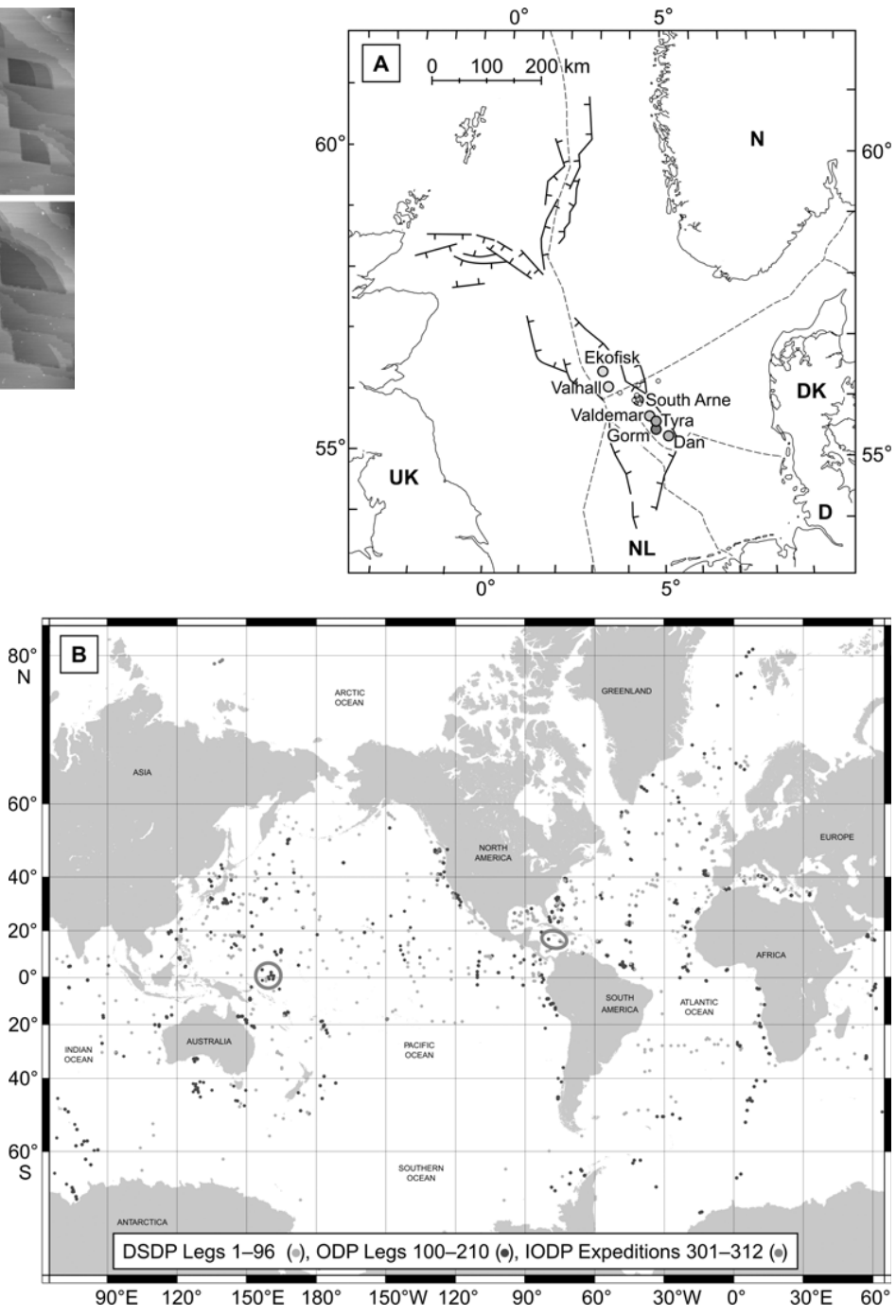


Fig. 5. (A) Sampled North Sea hydrocarbon bearing chalk fields. In addition to the hydrocarbon bearing chalk, water zone chalk was sampled (small dots) from Baron-2, I-1, Otto-1, Q-1, and T-3X near South Arne, and from Cecilie-1B, Gert-1, and West Lulu-1. (B) Sampled Ocean Drilling Program sites (http://iodp.tamu.edu/scienceops/maps/iodp-odp-dsdp2.pdf).

# Table 1. Previous studies on material used in the present paper

| *Locality* | *Author* | *Subject* |
|---|---|---|
| *The Ontong* | Lind *et al.* (1993) | Color bands in ooze |
| *Java Plateau* | Berger & Lind (1997) | |
| | Lind (1993a) | Stylolite formation |
| | Fabricius & Borre (2007) | |
| | Lind (1993b) | Mechanical compaction |
| | Audet (1995) | |
| | Urmos & Wilkins (1993) | Velocity and porosity depth-trends |
| | Urmos *et al.* (1993) | |
| | Fabricius *et al.* (in press) | |
| | Borre (1997) | Burial diagenesis, based on image analysis of back scatter electron micrographs |
| | Borre *et al.* (1997) | |
| | Borre & Fabricius (1998) | |
| | Borre & Fabricius (1999) | |
| | Gommesen & Fabricius (2001) | Elastic and static moduli as compared to Valhall and Tor fields. |
| | Fabricius (2003) | Review of burial diagenesis of chalk and presentation of the iso-frame model as a means to quantify chalk cementation from sonic data. |
| *The Caribbean Sea* | Lind (1997) | Sonic velocity |
| | Fabricius & Shogenova (1998) | |
| | Fabricius (2000) | Mechanical compaction |
| | Fabricius (2001) | |
| | Mutti (2000) | Diagenesis |
| | Fabricius (2003) | |
| *North Sea, Dan field* | Lind & Schiøler (1994) | Stylolites |
| | Lind & Grøn (1996) | |
| | Røgen & Fabricius (2002) | Microtexture and physical properties |
| | Fabricius *et al.* (2007b) | |
| | Fabricius (2003) | Iso-frame modeling |
| | Røgen *et al.* (2004) | Influence of porosity and fluid content on ultrasonic velocity |
| | Røgen *et al.* (2005) | |
| | Larsen & Fabricius (2004) | Water saturation normalized to pore surface, as derived from core data and well logs |
| *North Sea, Gorm field* | Lind *et al.* (1994) | Permeability |
| | Mortensen *et al.* (1998) | |
| | Borre (1998) | Ultrasonic velocities |
| | Borre & Fabricius (2001) | |
| | Larsen & Fabricius (2004) | Water saturation normalized to pore surface, as derived from core data and well logs |
| | Røgen *et al.* (2005) | Influence of porosity and fluid content on ultrasonic velocity |
| | Fabricius & Borre (2007) | Diagenesis |
| *North Sea, Tyra field* | Lind & Grøn (1996) | Microtexture and physical properties |
| | Fabricius *et al.* (2007b) | |
| | Madsen & Lind (1998) | Wettability |
| | Borre (1998) | Ultrasonic velocities |
| | Røgen *et al.* (2001) | Image analysis of electron micrographs |
| *North Sea,* | Prasad *et al.* (2005) | Petrophysical analysis |
| *Valdemar field* | Fabricius *et al.* (2005) | |
| *North Sea,* | | |
| *South Arne field* | Røgen & Fabricius (2002) | Microtexture and physical properties |
| | Fabricius *et al.* (2007b) | |
| | Fabricius (2003) | Iso-frame modeling of chalk |
| | Fabricius *et al.* (2007a) | |
| | Japsen *et al.* (2004) | Influence of porosity and fluid content on ultrasonic velocity |
| | Røgen *et al.* (2004) | |
| | Røgen *et al.* (2005) | |
| | Vejbæk *et al.* (2005) | |
| | Fabricius *et al.* (in press) | Relationship between burial stress and physical properties |
| *North Sea, Valhall field* | Gommesen & Fabricius (2001) | Elastic properties |
| | Røgen & Fabricius (2002) | Microtexture and physical properties |
| | Fabricius *et al.* (2007b) | |
| *North Sea, Ekofisk field* | Røgen & Fabricius (2002) | Microtexture and physical properties |
| | Fabricius *et al.* (2007b) | |
| *North Sea, Regional* | | |
| *chalk water zone* | Fabricius *et al.* (in press) | Burial stress and physical properties |

(Fig. 5; Hurst 1983; Brewster *et al.* 1986; Doyle & Conlin 1990; Farmer & Barkved 1999; Kristensen *et al.* 1995; Mackertich & Goulding 1999; Jakobsen *et al.* 2004). The North Sea data also comprise results from a study of the chalk water zone in the Northern part of the Danish sector of the Central North Sea (Fabricius *et al.* in press), whereas no outcrop data or data from hydrocarbon-bearing low-porosity chalk of the English sector is included. Chalk samples from the non-hydrocarbon-bearing deep sea oceanic plateaus are represented by material from the Ontong Java Plateau where chalk sediments are thick and from the Caribbean Sea where the chalk sediments are mixed with silicates (Kroenke *et al.* 1991; Sigurdsson *et al.* 1997).

# Data

Most data discussed in the present paper have already been reported and discussed in various contexts and published in the papers outlined in Table 1.

# Chalk composition

## Primary components

The main component of chalk is calcareous nannofossil mud of clay to silt size, frequently with admixtures of sand-size calcareous microfossils, so that chalk has a mudstone or wackestone microtexture, and less frequently a packstone microtexture. Grainstones occur rarely in the North Sea chalk and were also only rarely seen in the sediment cores from Ontong Java Plateau and the Caribbean Sea (Crabtree *et al.* 1996; Kroenke *et al.* 2001; Sigurdsson *et al.* 1997). In North Sea chalk larger calcareous fossils may be found intact or as represented by bioclasts. Entire calcareous macrofossils are a main reason for a macro-palaeontological interest in the chalk, but probably only rarely contribute to the overall physical properties of the chalk.

In addition to calcareous components, the chalk may contain remains of siliceous nannoplanton and microfossils, and chalk may vertically or laterally grade into diatomites or spiculites (Calvert 1974). In the North Sea chalk, remains of siliceous sponges are not uncommon (Maliva & Dickson 1992), and in the deep sea chalk phosphatic fossil remains are also seen (Fig. 2). Siliciclastic material and heavy minerals in chalk may be transported from the continent by wind or when the coast is not too far away, via rivers and via turbidites from delta-slopes. Another source of silicates is volcanic ash (Kroenke *et al.* 1991; Sigurdsson *et al.* 1997; Simonsen & Toft 2006).

In deep sea as well as North Sea chalk, most intervals are dominated by bioturbation, so that primary sedimentary structures are obscured although the overall composition indicates a "pelagic rain" mode of deposition (Ekdale & Bromley 1984). In some intervals sedimentary structures and particle sorting indicates that the sediment was transported or winnowed by traction currents (Herrington *et al.* 1991; Kroenke *et al.* 1991). In other intervals, the presence of chalk intraclasts indicates that the sediment was re-deposited by mass flow (Herrington *et al.* 1991; Kroenke *et al.* 1991; Damholt & Surlyk 2004).

The chalk may be bedded, typically on a decimeter to meter scale as visible from systematic variations in grayness or in degree of oil staining and as reflected in systematic variations in induration, porosity, silicate content and possibly depositional texture. The bedding may indicate deposition via turbidites, climatically controlled variations in plankton composition and influx of silicates, or may indicate intermittent deposition followed by sea floor diagenesis (Kroenke *et al.* 1991; Sigurdsson *et al.* 1997; Scholle *et al.* 1998; Henriksen *et al.* 1999; Damholt & Surlyk 2004).

## Diagenetic components

Diagenetic components may be the result of bacterial action, or they may be the result of chemical equilibration between minerals and pore water typically taking place during burial under increasing temperature. Where the carbonate ooze is relatively rich in organic material, as is typically the case near the shore, the results of bacterial action may dominate the diagenetic structures and mineralogy, whereas where the ooze is poorer in organic material, the result of chemical equilibration with pore water will dominate (see *e.g.* D'Hondt *et al.* 2003 on bacteria in pelagic sediments).

In newly deposited carbonate ooze, organic components are more or less preserved. They include the polysaccharides which formed a template for the growth of calcite within the living organism (Henriksen *et al.* 2004). The ooze is generally light brown. It thus contains organic material, which is a source of energy for macroscopic sediment feeders, whose burrowing activity leave behind trace fossils. It is also a source of energy for microorganisms whose activity may result in precipitation of minerals. Where the sea bottom for a period is left with no significant sedimentation, it is thus probably microbial action which is reflected in the formation of components which

are not seen in sediments dominated by burial diagenesis: glauconite, and phosphatic nodules, or in precipitation of carbonate in the ooze of the sea floor so that a hardground forms (Hancock 1975; Mutti & Bernoulli 2003).

In an environment with continuous sedimentation, bacteria clean away the organic coating of the sediment particles while the sediment is gradually buried. Some organic material may be left in the chalk (Bürki *et al.* 1982; Stax & Stein 1993), some of it possibly enclosed in crystals and thus protected from microorganisms. The action of sulphate reducing bacteria not only removes organic material, it also extracts iron and other heavy metals from volcanic ash, metal oxides, and clay, resulting in the formation of pyrite (Lind *et al.* 1993; Musgrave *et al.* 1993). The degradation of organic matter from siliceous fossils may release barium to the pore water, resulting in the precipitation or growth of barite, which already may nucleate in the sea water before sedimentation (Cronan 1974; Baker *et al.* 1982).

With removal of the organic coating on the fossils, chemical equilibration between the minerals constituting the fossils and other components of the sediment and the pore water can take place. Low-magnesium calcite recrystallizes and fossils of high-magnesium calcite and aragonite will dissolve and release not only calcium and carbonate ions but also magnesium and strontium among other metal ions to the pore water. The released Mg may precipitate in dolomite (Hancock 1975). Dolomite was found in North Sea chalk (Fig. 1), but not in chalk from Ontong Java Plateau, probably as a reflection of the absence of high magnesium carbonate in the deep sea ooze. The released strontium may be incorporated in barite or form celestite (Delaney & Linn 1993; Lyons *et al.* 2000, Fabricius & Borre 2007).

If the transport of water through the sediment is negligible (as is probably the case in chalk during burial (Jørgensen 1987)), the recrystallization of calcite causes oxygen and carbon isotopes of the solid phase to equilibrate with the carbon and oxygen isotopes of the dissolved bicarbonate and the oxygen of the water. When temperature increases, the tendency for the solid phase to prefer the heavier isotopes diminishes, but because the solid phase contains much more carbon than the pore water, the carbon isotopes of the solid will not change much during this process. In highly porous sediments, the pore water contains more oxygen than the solid phase and it will have a large influence on the isotope ratio of the calcite, which progressively loses $O^{18}$, as reflected in a lowering of $\delta^{18}O$ with increasing temperature and burial (Fig. 6; Jørgensen 1987). The decline in $\delta^{18}O$ takes place at shallower depth in the Caribbean Site 999 than at Site 807 in the Ontong Java Plateau, probably as a reflection of the high content of volcanic ash, which incorporates $O^{18}$ from the pore water during its diagenesis to smectite (Lawrence & Gieskes 1981).

At the time of deposition siliceous fossils are composed of opal-A, which has a relatively high solubility, so that with removal of the organic coating during burial, opal-A equilibrates with pore water of a relatively high Si-concentration. If siliceous fossils are rare they may go totally into dissolution and leave molds behind. As the sediment ages and when the temperature increases as a consequence of burial, opal-CT becomes the dominating silica phase (Fig. 6). Opal-CT is in equilibrium with pore water with a lower Si-concentration than opal-A, so it may now precipitate as sub-micron-size aggregates floating in water of pores or open fractures and gradually cause all opal-A to disappear. At this stage, in silica rich beds or fractures (Madirazza 1965), burial-diagenetic chert may form in equilibrium with the pore water. At still deeper burial opal-CT transforms to quartz and the Si-concentration in the pore water equilibrates at a still lower level (Kastner 1981; Maliva & Dickson 1992).

In an environment rich in organic matter, pyrite and sulphates may via microbial action grow as concretions. Opal may also, possibly under microbial action, dissolve and reprecipitate, forming chert concretions. Although it has been suggested that chert formation involves redox-reactions and pH-gradients in the pore water (*e.g.* Clayton 1986) it may be simpler to invoke direct microbial involvement in the precipitation. Concretions grow at the expense of calcite in the host chalk (Maliva & Siever 1989; Dewers & Ortoleva 1990). Chert may in this environment form at modest burial in a sediment rich in siliceous fossils (Hancock 1975).

Silicates in the chalk are predominantly clay minerals (Lindgreen *et al.* 2002). The shallowest deep sea samples from Ontong Java Plateau (ODP Site 807) and the Caribbean Sea (ODP Sites 999 and 1001) contain predominantly mixed smectite-chlorite, probably derived from volcanic ash. With depth it gradually recrystallizes to pure smectite, while releasing iron to the pore water and incorporating Mg (Fabricius & Borre 2007). In ODP Site 999, smectite was also provided to the sediments from a continental source, probably by distant turbidites from a river delta deposit (Sigurdsson *et al.* 1997). With depth the smectite is replaced by mixed smectite-illite (Fig. 6). For the studied North Sea samples a depth wise change in clay mineralogy is observed: from smectite-illite via illite-smectite to smectite-chlorite (Fig. 6). This trend is reflected in the different chalk fields:

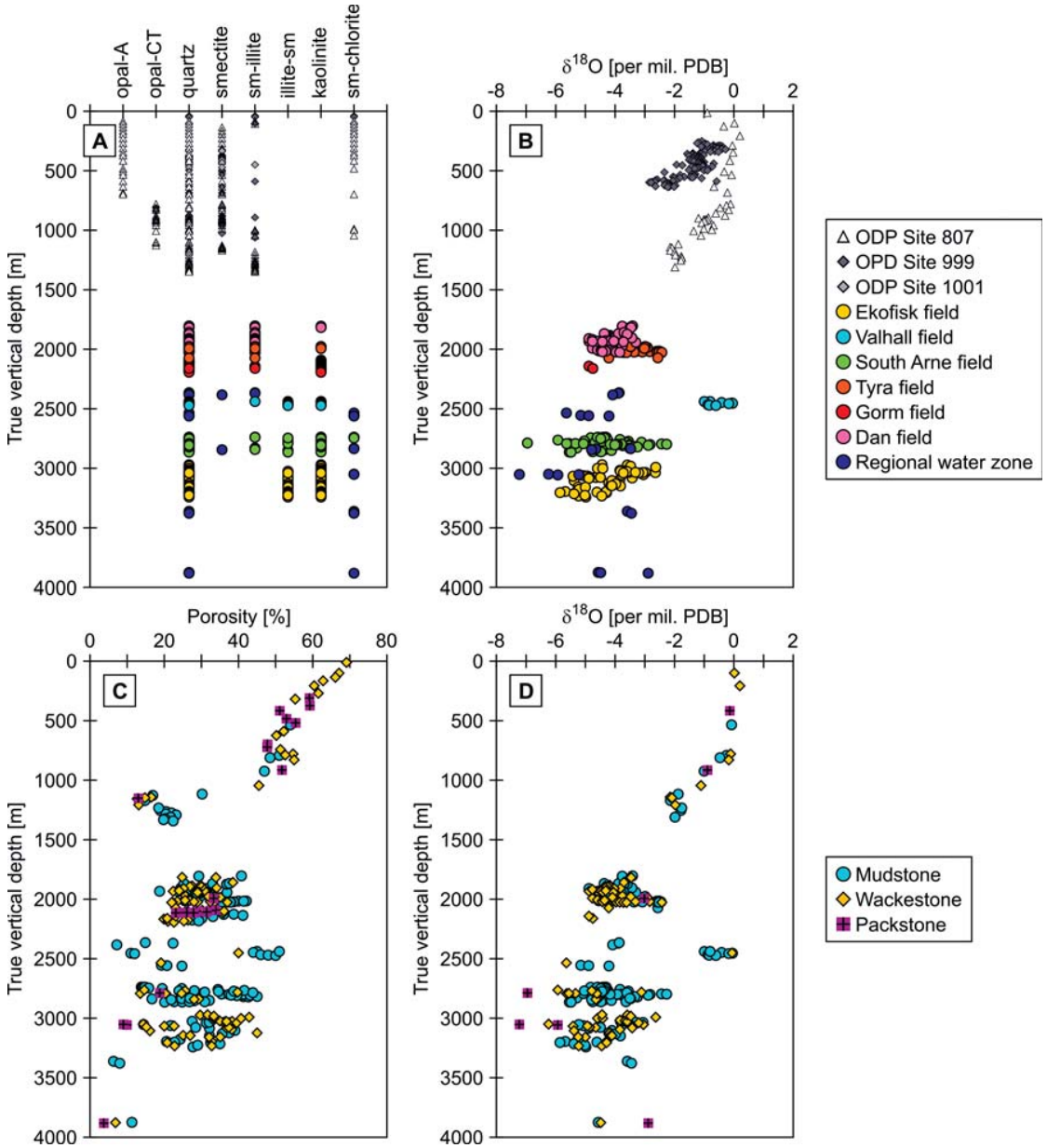


Fig. 6. Regional depth trends in mineralogy, stable oxygen isotope ratios, and porosity. For the deep sea samples where water depth is on a km scale, the depth is given with reference to the sea floor. For North Sea samples, the depth is relative to mean sea level, but because the North Sea is so shallow (less than 100 m), the depth scales are roughly comparable. Figures (A) and (B) are annotated with respect to locality and also chalk samples with less than 90% carbonate are included. Figures (C) and (D) are annotated with respect to micro-texture and only samples where micro-texture is known are included.

the Dan field samples mainly contain smectite-illite, the deeper Ekofisk field mainly illite-smectite, whereas smectite-chlorite is found in the deep water zone samples. In the South Arne field, kaolinite was found both as detrital clasts and as precipitate in the pores, possibly formed at the expense of dissolved feldspar (Fabricus *et al.* 2007a). Clay minerals may upon recrystallization remain disseminated in the sediment or form stylolites or diagenetic flaser structures (a network of anastomozing microstylolites) as a reflection of the original distribution of clay (Lind 1993a; Fabricius & Borre 2007). In bedded chalk, stylolites may thus be relatively frequent in intervals with low porosity (Scholle *et al.* 1998). In addition to clay minerals, zeolites and feldspar may precipitate in the

chalk as a result of burial diagenesis (Kastner 1981; Williams & Crerar 1985; Williams *et al.* 1985; Fabricius & Borre 2007).

### Porosity

At the sea floor, newly deposited calcareous ooze has porosity around 70% and water is thus the main component (Fig. 6). The porosity of the newly deposited sediment is interparticle porosity between the sediment grains and intraparticle porosity within shells of microfossils as foraminifers and radiolaria. The studied samples are from the central North Sea and deep sea plateaus where continuous burial is generally the rule and hardground formation is rare. Under these conditions porosity declines as a consequence of the load of the increasing overburden concurrent with isotopic equilibration between porewater and sediment (Fig. 6). Down to below 800 m the microfossils remain hollow and we find a relatively narrow porosity-depth trend irrespective of chalk texture (Fig. 6). This is because the intrafossil porosity is largely balanced by the contribution to the solid from the fossil shell (Borre & Fabricius 1999; Fabricius & Borre 2007).

After the onset of stylolite formation below 800 meters of depth (Lind 1993a), pressure dissolution presumably adds calcium and carbonate ions to the pore water and pore-filling cementation takes place. The porosity shifts to a lower level, but varies from less than 20% to more than 40% at the same burial depth. Microfossils and molds become filled with carbonate cement, and the depositional texture is now to some extent reflected in the porosity (Fig. 6), but the pattern is complicated by the grain size distribution in the carbonate mud. Where the mud is well sorted and dominated by silt-size nannofossil remains, the porosity will be relatively high, but the porosity will be relatively low where a clay-size component of detrital and diagenetic clay minerals, diagenetic silica or fine nannofossil debris is admixed (Lind & Grøn 1996; Borre & Fabricius 1999; Røgen *et al.* 2001; Røgen & Fabricius 2002; Fabricius & Borre 2007; Fabricius *et al.* 2007b).

Re-deposited, clast-bearing chalk have in some cases been found to have relatively high porosity (Hatton 1986; Fabricius *et al*. in press), probably as a reflection of a mudstone microtexture and sorting of the mud matrix related to the depositional mechanism. Fabricius & Borre (2007) found samples of redeposited chalk from the Ontong Java Plateau to have relatively high mud matrix porosity, although the total porosity of these samples was low when the content of cemented microfossils was high. In other cases clast-bearing and clearly re-deposited chalk was not found to be anomalously porous (Herrington *et al.* 1991; Fabricius *et al.* 2007b). In line with these observations Maliva & Dickson (1992) found no direct link between porosity and mode of deposition of chalk in the Eldfisk Field. They found a better correlation between content of non-carbonates and porosity.

In hydrocarbon-bearing chalk, depth-wise porosity reduction tends to be arrested, so that porosity remains high for a given burial depth (Fig. 6; Scholle 1977). Valhall samples have a high $\delta^{18}O$ relative to burial depth. This indicates introduction of hydrocarbons at shallow burial (Fig. 6), because where a large part of the pore space is taken up by hydrocarbons, only little water is present, and $\delta^{18}O$ must remain high. For the remaining samples, $\delta^{18}O$ declines until around 2800 m burial; but a depth-wise porosity reduction is only obvious in the ODP-samples (to around 1000 m depth). This indicates a temperature (depth) control on $\delta^{18}O$, but that porosity-reduction is not directly controlled by temperature (Fabricius *et al.* in press).

## Burial diagenetic porosity reduction in chalk

Porosity reduction during burial takes place by two mechanisms: mechanical compaction, and pore filling cementation. Both are linked to the drainage history and the stress caused by the load of the overburden – mechanical compaction directly, pore filling cementation indirectly via pressure dissolution at stylolites.

### Mechanical compaction of chalk

Geotechnical loading experiments on chalk from outcrops around the North Sea, on North Sea reservoir cores, and on deep-sea cores designate mechanical compaction to be the major porosity reducing agent down to porosities of 50% in and some cases even to 40% (Jones *et al.* 1984; Ruddy *et al.* 1989; Lind 1993b; Fabricius 2000, 2001, 2003). The governing stress is the highest experienced effective stress, $\sigma'$, as defined by Terzaghi (1923):

$$\sigma' = \sigma - U \quad (1)$$

where $\sigma$ is the total load of the overburden and U is the pore pressure. The mechanical compaction is the effect of the stress-dependent consolidation and the

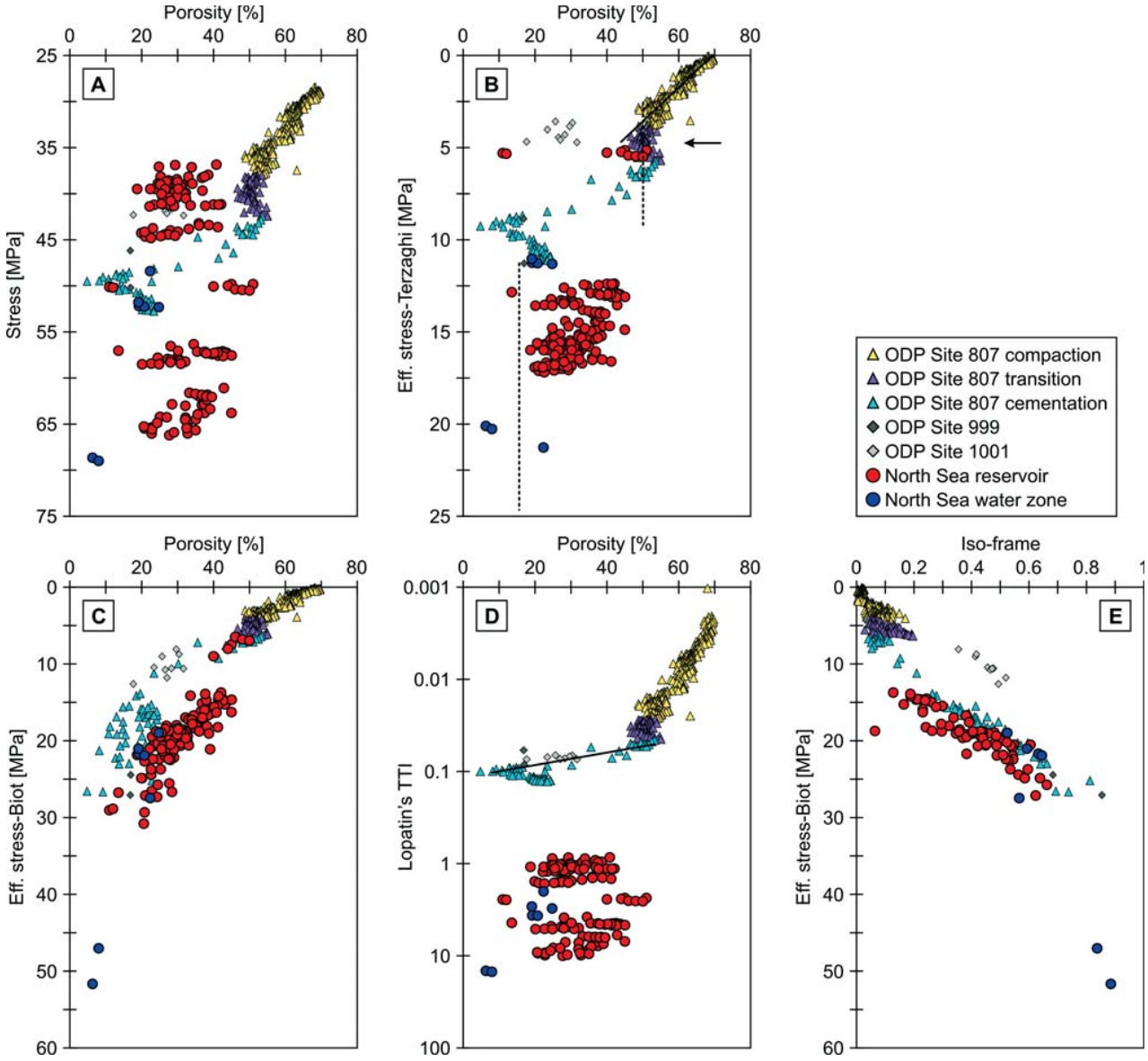


Fig. 7. Effect of stress and temperature on diagenesis as reflected in porosity and iso-frame value. Iso-frame value is a number describing pore-stiffness on a scale from 0 to 1 as modeled from sonic velocity, mineralogy and porosity. Samples all represent >90% carbonate. The temperature is represented by Lopatin´s time-temperature index TTI. The depth axis of Fig. 6 is now replaced by respectively total stress, effective stress calculated according to Terzaghi's law, TTI, and effective stress calculated by taking Biot's coefficient into account (Refer Fig. 11), Because the chalk commonly may be assumed to be water wet, the pressure in the water phase has been used in the present calculations, but if for arguments sake, the (higher) pressure in the hydrocarbon phase is used, the change in pattern is barely visible (Fabricius *et al.* in press). The solid line in (B) represents the effective stress interval of mechanical compaction, the stippled lines represent intervals of only limited porosity reduction. The solid line in (D) represents TTI of pore-filling cementation in the cold deep sea settings, probably reflecting the transition from opal-CT to quartz, which causes concentration of Si in pore water to drop, and Ca to be released from silicate-complexes. The arrow in (B) represents the onset of pressure dissolution and consequent cementation in warm (North Sea) settings, where a TTI sufficient for opal-CT – quartz transition has already been met at lower effective stress.

time-dependent creep (Krogsbøll & Foged 2003). When this is taken into consideration, pre-consolidation may be estimated from consolidation data, and it can be deduced at which effective burial depth mechanical compaction was arrested in a given setting (Fabricius 2000, 2003).

When rather than depth, total burial stress, $\sigma$, is plotted versus porosity, the gap between ODP and North Sea samples disappears due to the weight of the deep water at the ODP localities (Fig. 6C, 7A). In the Chalk Group of the central North Sea, the pore pressure is significantly higher than hydrostatic, probably because a rapid Cenozoic subsidence and sediment deposition has prevented drainage equilibrium and thus caused the building up of pore-pressure (*e.g.* Japsen 1998). This over-pressure varies regionally, so in order to interpret the porosity decline, it is the effective stress rather than the total stress which must be plotted against porosity, and a mechanical compaction trend down to a $\sigma'$ of ca. 4 MPa becomes apparent (Fig. 7B; Gommesen & Fabricius 2001).

The mechanical compaction may occur concurrently with the time- and temperature-dependent recrystallization of the calcite as deduced from chemical data by Baker *et al.* (1982) and from petrography and image analysis by Borre & Fabricius (1998). It must be emphasized that recrystallization is not in itself porosity-reducing, although the smoothening of particles may further the mechanical compaction (Borre & Fabricius 1998).This is also reflected in the modeling results of Audet (1995) although he did not mention the possibility.

Even when recrystallization of calcite has caused the calcite particles to form interfaces in the form of contact cement, mechanical compaction may still occur if loading resume after an intermission under normal burial conditions, or where hydrocarbon production has lead to the lowering of pore pressure and consequent increase in effective stress. In these cases mechanical compaction involves breaking crystals or probably more easily the contact cement and thus involves forcing the water molecules that bridge the crystal faces to detach from one face. This process apparently is relatively easy when the pores are saturated with water, which is a polar fluid, so that water is available to ensure that the surface charges on the exposed crystal face are neutralized. If a polar fluid is not available, electrical forces will work against the breakage. Mechanical tests have consequently shown that compaction requires higher stress when the saturating fluid is less polar, so that oil-saturated or dry chalk can withstand more stress than water saturated chalk (Risnes 2001; Risnes *et al.* 2005).

Several workers have discussed this phenomenon of "water weakening", and several alternative mechanisms have been proposed. Some authors attribute the phenomenon to surface tension between *e.g.* air and water resting as menisci around grain contacts of a partially saturated chalk (Delage *et al*. 1996), but this mechanism does not explain the stiffness of oil-saturated chalk. Other authors invoke pressure dissolution at calcite grain contacts (Hellmann *et al.* 2002), although pressure dissolution would supposedly strengthen rather than weaken the rock, as it causes an increase in the crystal-crystal contact area. Also more purely chemical mechanisms have been suggested, where Ca-ions adsorbed to the calcite at grain contacts cause a net diffusion of Ca-ions away from the contacts due to electrical repulsion, and thus dissolution at contacts (Heggheim *et al.* 2005). This setting would though rather lead to a stable condition where relatively few Ca-ions adsorb to the calcite near grain contacts.

## Cementation in chalk

Depending on natural loading rate, the mechanical compaction is at some stage halted by the contact cement. A cementation front involving pore-filling cementation may occur immediately –as is the case in ODP Sites 999 and 1001, or after a transition interval at a higher effective stress as is the case in ODP Site 807 (Fig. 7B, 8B; Fabricius 2000). Micro-stylolites or flaser structures were found from 572 meters below sea floor in the Caribbean Site 999 corresponding to an effective stress of ca. 4.5 MPa and are directly correlated with the onset of pore-filling cementation. In Site 807 from the Ontong Java Plateau, microstylolites were observed from a depth of 490 meters below sea floor at an effective stress of ca. 3 MPa, proper stylolites from a depth of 830 meters below sea floor, corresponding to an effective stress of ca. 5.7 MPa, but the cementation front was not observed until an effective stress of 6.6 MPa. The discrepancy between the two sites indicates that dissolution at stylolites and precipitation of cement are controlled by different mechanisms (Fabricius 2000).

That formation of stylolites is controlled by effective stress rather than temperature, burial depth or total stress is indicated by the North Sea data. Stylolites were not observed in the sampled interval of the cores from Valhall, which are relatively deeply buried, but are under a relatively low effective stress; whereas stylolites were noted in less deeply buried chalk of similar age and texture in the Dan, Gorm and Tyra fields (Fig. 8A, B). On the other hand, in silicate-rich cold deep sea chalk of the Caribbean sites 999 and 1001, microstylolites were noted at lower

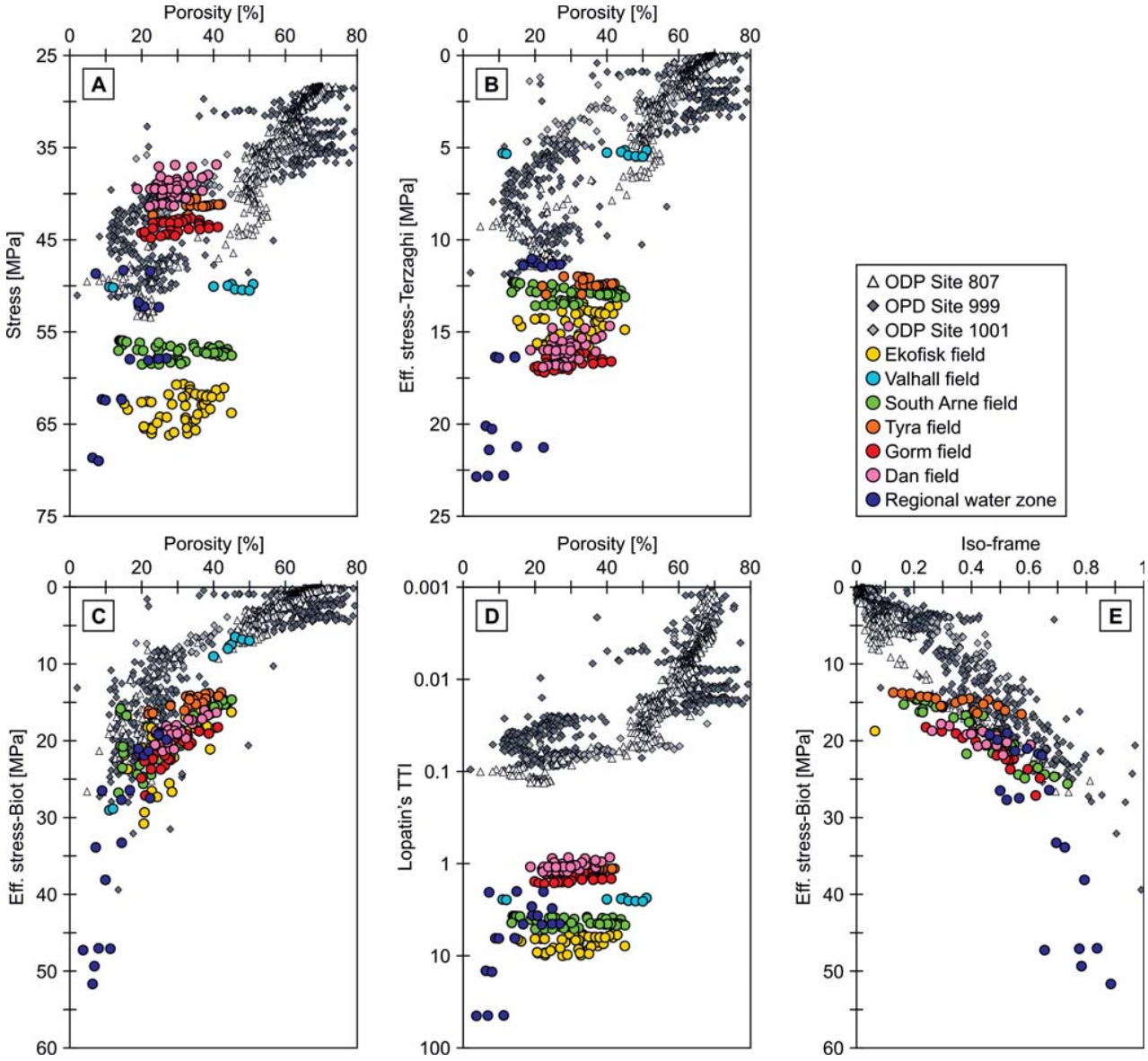


Fig. 8. Porosity and iso-frame values vs. stress and TTI corresponding to Fig. 7. Here all chalk samples are included, irrespective of carbonate content.

effective stress than experienced in the pure Valhall section (Fig. 8B).

The source of cement is thus assumed to be pressure dissolution at the clay-calcite interface in a stylolite, rather than at calcite-calcite interface. Pressure dissolution at calcite-calcite interfaces was postulated by Scholle (1977) although he noted that he saw no petrographic evidence in chalk, similarly Maliva & Dickson (1992) studied chalk from the Eldfisk field and only found little evidence of intergranular pressure dissolution and found stylolites to be the major source of cement. Lind & Schiøler (1994) found that the clay drape of stylolites from the Dan field has different composition from the clay dispersed in the chalk, indicating that stylolites form at distinctive pre-cursers as for example ash beds or clay beds. Calcium and carbonate ions released by pressure dissolution at stylolites do not preferably precipitate in the immediate neighborhood of stylolites (Fig. 1, 2; Lind 1991; Lind & Grøn 1996). On the other hand, a link between pore-filling cementation and the presence of stylolites implies that silicate-poor intervals with rare stylolites may stay porous even where no hydrocarbons are present until stress is high enough for calcite-calcite pressure dissolution. Experiments by Zubtsov *et al.* (2005) indicate than pressure disso-

lution of calcite crystals requires stress above 50 MPa, corresponding to a burial depth of around 5 kilometers.

Precipitation of cement is a chemical process and may be linked to a reaction requiring activation energy. It should thus be correlated to the time –temperature index of Lopatin, TTI (Waples 1980) which describes the cumulative effect of the time a sedimentary rock experiences in each 10° temperature interval during burial. Pore-filling cementation does indeed seem to take place in a narrow TTI interval in pure chalk (Fig. 7D), and at a lower TTI in the silicate rich chalk (Fig. 8D). The controlling chemical process is though hardly precipitation of calcite, as it takes place readily during recrystallization. Indeed a more likely candidate is the transition from opal-CT to quartz, because it depends on tempertature and time and because it will change the concentration of Si in the pore water (Kastner 1981). The mechanism is that a relatively high concentration of Si maintains an apparent super-saturation of Ca in the pore water via formation of aqueous complexes (Fabricius & Borre 2007). Accordingly, in both ODP Site 999 of the Caribbean Sea and ODP Site 807 of the Ontong Java Plateau, the calcite cementation front concurs with a drop in Si in the pore water (Lyons *et al.* 2000; Fabricius & Borre 2007).

An apparent supersaturation of Ca in the pore water of chalk has been explained in alternative ways. It was attributed to an affect of magnesium ions (Neugebauer 1974), but a reduction in Ca-activity due to the presence of Mg is not enough to explain the apparent supersaturation, and the presence or potential presence of a Mg-bearing calcite phase has been postulated (Berner 1975; Fabricius 2003), but was not noted by electron microscopy of chalk. The presence of organic coating on some coccoliths (Bürki *et al*. 1982) would not cause super saturation of calcite, as it would not hinder precipitation on uncoated crystals.

Below the cementation front, porosity is stable or vanes quietly (Fig. 6C, 7A,B,D, 8A,B,D). It is obvious though that hydrocarbons have a positive effect on porosity preservation, such that water zone chalk has lower porosity than chalk from the hydrocarbon bearing fields (Fig. 8). It is characteristic that water leg samples from the fields plot on trend with regional water zone data (Fig. 8; Andersen 1995). The hydrocarbon bearing intervals have water as well as oil in the pores, and when the water content is normalized to area of the pore-surface, a pseudo water film thickness can be derived (Engstrøm 1995), which is 1) more than sufficient to cover the pore walls, 2) forms a rough gradient with depth as a reflection of capillary pressure, 3) compares with mercury-air capillary curves recalculated and normalized to water film thickness (Larsen & Fabricius 2004; Fabricius *et al.* 2005; Fabricius *et al.* 2007a). The water saturation at high capillary pressures is thus not constant, and an irreducible zone where continuity in the wetting phase is lost (Anderson 1987) has not been reported in the chalk reservoirs.

The hydrocarbon effect may be caused by several factors, including inhibition of pressure dissolution, slow diffusion in the water phase, and adsorption of polar hydrocarbons to the calcite surface inhibiting precipitation of calcite. Although polar hydrocarbons adsorb readily on calcite surfaces in a hydrocarbon medium (*e.g.* Madsen *et al.* 1996; Madsen *et al.* 1998), and polar hydrocarbons adsorb readily from air (Stipp 2002), polar hydrocarbons that are soluble in water adsorb more readily on silicates than on calcite (Madsen & Lind 1998; Clausen *et al.* 2001), so it is possible that the hydrocarbon effect is caused by adsorption of hydrocarbons to the stylolites and consequent choking of the pressure solution process (Fabricius 2003). Hydrocarbon bearing chalk may be extensively recrystallized, indicating chemical equilibration via diffusion in the pore water even in hydrocarbon bearing intervals (Fig. 3B).

## Elastic properties of chalk

The elastic properties of a linear elastic material may be described by elastic moduli (Fjær *et al.* 1992; Mavko *et al.* 1998). The bulk modulus, K, describes the ratio of hydrostatic stress, $\sigma_0$, to volumetric strain, $\varepsilon_0$:

$$K = \sigma_0/\varepsilon_0 \quad (2)$$

Because the strain signifies the relative change in volume it has no unit, so K and the other elastic moduli will have the unit of pressure or stress, typically GPa.

The shear modulus, G, describes the ratio of shear stress, $\sigma_s$, to total shear strain, $\gamma$:

$$G = \sigma_s/\gamma \quad (3)$$

The ratio of uniaxial stress, $\sigma$, to uniaxial strain, $\varepsilon$, under the condition that no deformation is possible in directions perpendicular to the stress, i.e. conditions found in a sedimentary basin, is called the Oedometer modulus, M:

$$M = \sigma/\varepsilon \quad (4)$$

When sound waves propagate through an elastic medium, the velocity of pressure waves, $v_P$, and shear

waves, $v_S$, is determined by the bulk density of the material $\rho_b$ and the elastic moduli:

$$v_P^2 = M/\rho_b \quad (5)$$

$$v_S^2 = G/\rho_b \quad (6)$$

M is in this context referred to as P-wave modulus.

Sedimentary rocks like chalk are porous media and composites of solid and pore-fluid. Water saturated chalk is mainly composed of calcite and water, and dry chalk is mainly composed of calcite and air. The bulk density will thus be larger for water saturated than for dry chalk:

$$\rho_b = \rho_{calcite}\,(1-\phi) + \rho_{pore}\,\phi \quad (7)$$

where $\rho_{calcite}$ is density of calcite, $\phi$ is porosity, and $\rho_{pore}$ is density of pore fluid. In hydrocarbon reservoirs the pore fluid will typically be a heterogeneous mixture of hydrocarbons (oil or gas) and saline water.

Because it is a porous rock, chalk is not a linear elastic medium, and when a stress is applied to chalk it will tend to deform plastically by porosity reduction already before the stress level of pore-collapse where mechanical compaction becomes dominating (Andersen 1995; Krogsbøll & Foged 2003). However, for deformation by sound waves (dynamic deformation) the permanent deformation is insignificant and we may assume linear elasticity in the dynamic case. It has been a general observation that elastic moduli for chalk as measured by geotechnical methods (static deformation) are smaller than would be expected from sonic velocity and density (Schön 1996; and *e.g.* Henriksen *et al.* 1999; Gommesen & Fabricius 2001). The apparent difference though may be due to experimental difficulties (Olsen *et al.* in press a) and in the following discussion it is assumed that P-wave modulus, M, calculated from $v_P$ and $\rho_b$ is an upper bound for undrained Oedometer modulus, M, corresponding to elastic deformation in the sedimentary basin.

## Modeling of elastic properties of chalk

Interpreting sonic velocity in carbonates may give useful information on composition; porosity, and pore structure (Castagna *et al.* 1993; Lind 1997; Fabricius & Shogenova 1998; Anselmeti & Eberli 2001; Prasad *et al.* 2005), but modeling of sonic velocity requires reference to the elastic parameters, because it allows the use of the laws of mechanics. One purpose of modeling is to optimize the prediction of sonic velocity from density or from porosity and vice versa (Hvid, 1998; Walls *et al.* 1998; Anderson 1999; Henriksen *et al.* 1999; Jacobsen *et al.* 1999; Japsen *et al.* 2004). Another purpose is to interpret the effect of composition of the pore fluid on velocity- and density data (Megson 1992; Borre *et al.* 2004; Japsen *et al.* 2004; Røgen *et al.* 2004; Gommesen *et al.* 2007).

When modeling a set of data, it is thus commonly a goal to optimize the match between data points and a curve in *e.g.* the density – bulk modulus plane. However, if we wish both to predict sonic velocity from density, and achieve information on *e.g.* degree of cementation, we need to construct a more rigorous physical model. This may be done in different ways: by modeling grain contacts (Dvorkin *et al.* 1994) or by effective media modeling of discrete pores in a solid (Berryman 1980), or of mixtures of suspended solids in spherical pores in a solid (Fabricius 2003). For a comparison of different chalk models refer to Røgen, *et al.* (2004); Gommesen *et al.* (2007); Olsen *et al.* (in press b).

An effective medium model which is designed for chalk is the iso-frame model (Fabricius 2003; Fabricius *et al.* 2007a). It is based on the model of Hashin & Shtrikman (1963). These authors defined bounds for the elastic moduli of mixtures of two components. The bounds are modeled as hollow spherical shells of one component of a continuum of sizes filling out the space, where the other component fills the spheres. The relative thickness of the walls of the spherical shells is defined from the amount of each component. The upper bound thus refers to the case where the component with highest shear modulus forms the spherical shells, the lower bound where the component with lowest shear modulus forms the spherical shells. The thick outer curves on Fig. 9 refer to the Hashin-Shtrikman bounds for P-wave modulus and shear modulus of mixtures of calcite and water and calcite and air. The lower bound for P-wave modulus corresponds to a suspension of calcite in water or air and is extremely low for mixtures of calcite and air. As porosity approaches zero, the lower bound becomes undefined. The lower bound for shear modulus is zero for mixtures with fluid or air because fluids have a shear modulus of zero.

In the iso-frame model the space between the bounds of Hashin & Shtrikman is filled by iso-frame curves. Each of the curves is defined as an Hashin-Shtrikman upper bound for a mixture of a solid and a suspension, where a constant part of the solid is in suspension and the remaining part (IF) is in the frame. In the simple case of one solid and one fluid, the model is formulated as:

$$K = \left( \frac{\phi + (1-IF)(1-\phi)}{K_{sus} + \frac{4}{3} G_{calcite}} + \frac{IF(1-\phi)}{K_{calcite} + \frac{4}{3} G_{calcite}} \right)^{-1} - \frac{4}{3} G_{calcite} \quad (8)$$

and for and for the shear modulus G:

$$G = \left( \frac{\phi + (1-IF)(1-\phi)}{\zeta} + \frac{IF(1-\phi)}{G_{calcite} + \zeta} \right)^{-1} - \zeta \quad (9)$$

$$\zeta = \frac{G_{calcite}}{6} \cdot \left( \frac{9 K_{calcite} + 8 G_{calcite}}{K_{calcite} + 2 G_{calcite}} \right) \quad (10)$$

and where for wet samples:

$$K_{sus} = \frac{\phi + (1-IF)(1-\phi)}{\left( \frac{\phi}{K_{water}} + \frac{(1-\phi)(1-IF)}{K_{calcite}} \right)} \quad (11)$$

whereas for dry samples:

$$K_{sus} = K_{air} \quad (12)$$

The P-wave modulus then becomes:

$$M = K + 4/3\ G \quad (13)$$

The iso-frame model may be formulated with the critical porosity concept and with any number of phases (Fabricius *et al.* 2007a). The critical porosity for chalk is typically 70%, corresponding to sea bottom porosity (Fig. 6C). By using critical porosity as an endpoint, the iso-frame model becomes less physically rigorous, but the isoframe-value calculated from different moduli gives a good match (Røgen *et al.* 2004, Olsen *et al.* in press b).

Iso-frame modeling can be done from porosity and one elastic modulus. The compiled chalk data indicate that P-wave moduli for water saturated (wet) or dry samples give similar IF, while wet G tends to indicate 0.05 higher IF and dry G 0.1 higher IF. The discrepancy still allows a good prediction of *e.g.* dry bulk modulus from wet M. The discrepancy may be inherent in the model, but it should be noted that when the difficulty of achieving 100% water saturation, and when the uncertainty of how to predict the elasticity of a mixed pore fluid is taken into account, IF from wet G is not significantly different from IF from wet or dry M (Fabricius *et al.* 2007a). These observations though, do not solve the problem of high IF from dry G. It is a possibility that the relatively high shear modulus of dry sedimentary rock is linked to the relatively high pore collapse stress of dry rock and thus possibly to the apparent high shear strength of the water film bridging the cemented interfaces of the dry chalk.

Low porosity samples from ODP Site 807 tend to have lower IF than low porosity North Sea samples, and samples from Valhall and South Arne fields have relatively high IF for a given porosity (Fig. 9). The iso-frame value gives a measure of cementation or pore-stiffness for a given porosity. Because it is formulated as a proportion of the solid, it is easy to visualize in log-interpretation (Fig. 10; Fabricius *et al.* 2005; Fabricius *et al.* 2007a).

## Biot's coefficient and effective burial stress

Because it is a measure of pore stiffness, the iso-frame value is closely related to Biot's coefficient (Olsen *et al.* in press b). Biot's coefficient, β, describes the ratio of pore volume change to bulk volume change during hydrostatic deformation. It may be expressed as:

$$\beta = (1 - K_{dry}/K_o) \quad (14)$$

where $K_{dry}$ is drained (equivalent to dry) bulk modulus of the rock and $K_o$ is mineral bulk modulus (Biot & Willis 1957). β falls in the range between porosity and one:

$$\phi < \beta < 1 \quad (15)$$

Under purely elastic and isotropic conditions $K_{dry}$ may be calculated from the velocities, $v_{Pd}$ and $v_{Sd}$, and density, $\rho_d$, of the dry rock:

$$K_{dry} = v_{Pd}^2 \rho_d - 4/3\ v_{Sd}^2 \rho_d \quad (16)$$

For pure chalk $K_o$ is ideally equal to $K_{calcite}$ and has a value of 71± 6 GPa (citations in Mavko *et al.* 1998). For less pure chalk $K_o$ may be modeled from the solid components of the chalk, although equation 14 strictly speaking is defined for a mono-mineralic solid (Gommesen *et al.* 2007). Where $\rho_b$, $v_P$ and $v_S$ are known for fluid saturated chalk, $K_{dry}$ may be estimated via Gassmann substitution (Gassmann 1951). Where only $\rho_b$ and $v_P$ are known, as is the case for the samples from the deep sea plateaus, $K_{dry}$ may be estimated via iso-frame modeling (Fabricius *et al.* in press).

With increasing pore stiffness, Biot's coefficient decreases while iso-frame value increases, so the compiled chalk data show that pores tend to stiffen with declining porosity (Fig. 9, 11). The data also show that samples from Valhall and South Arne tend to be relatively stiff for a given porosity, indicating the effect of pore-stiffening, porosity-preserving ce-

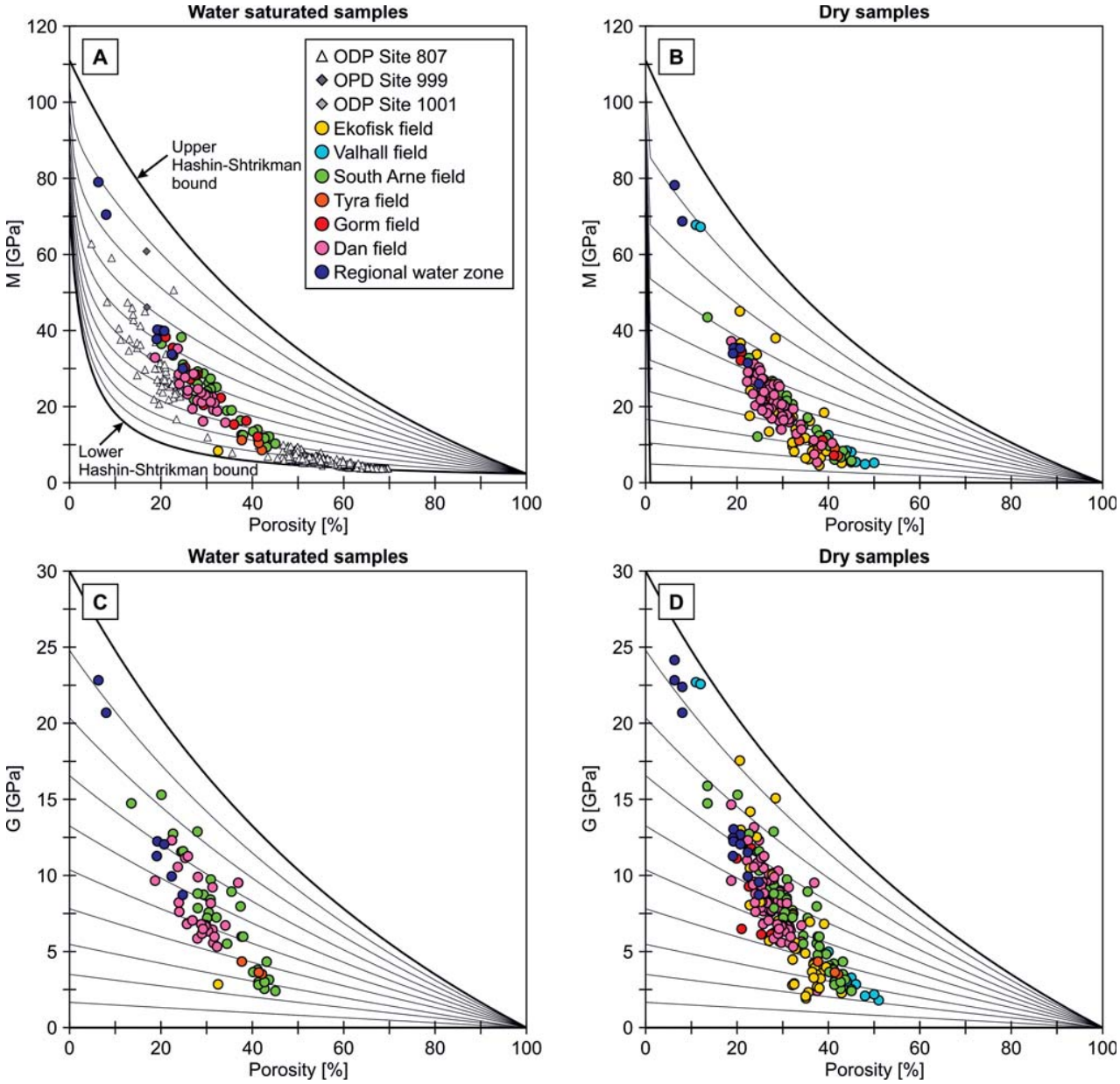


Fig. 9. Elastic moduli versus porosity for water saturated and dry chalk. All samples are chalk with more than 90% carbonate. (A), (B) P-wave modulus, M, as calculated from P-wave velocity and density. (C), (D) Shear modulus, G, as calculated from S-wave velocity and density. Water saturated M include data from ODP, mainly Site 807. G and dry M only include data from the North Sea. On each figure, iso-frame curves are shown in intervals of 0.1 ranging from 0 (lowest) to 1 (uppermost curve).

mentation, probably taking place after petroleum introduction (Fig. 9, 11). Warpinsky & Teufel (1992) found that β calculated from density and sonic velocities tends to be lower than when measured by geotechnical experiments.

Terzaghi´s effective stress law (eq. 1), may in the isotropic case be reformulated as:

$$\rho' = \rho - \beta U \quad (17)$$

(for a discussion see Nur & Byerlee 1971). The equation describes how as cementation increases, the pore pressure will be less effective in counteracting the outer stress. Although the stress law only applies strictly under ideal conditions, it may be used to discuss the effect of burial diagenesis (Fig. 7, 8). When effective stress is calculated by taking Biot's coefficient into account, the porosity decrease with stress follows a smooth trend for samples from water saturated chalk, whereas samples from hydrocarbon-

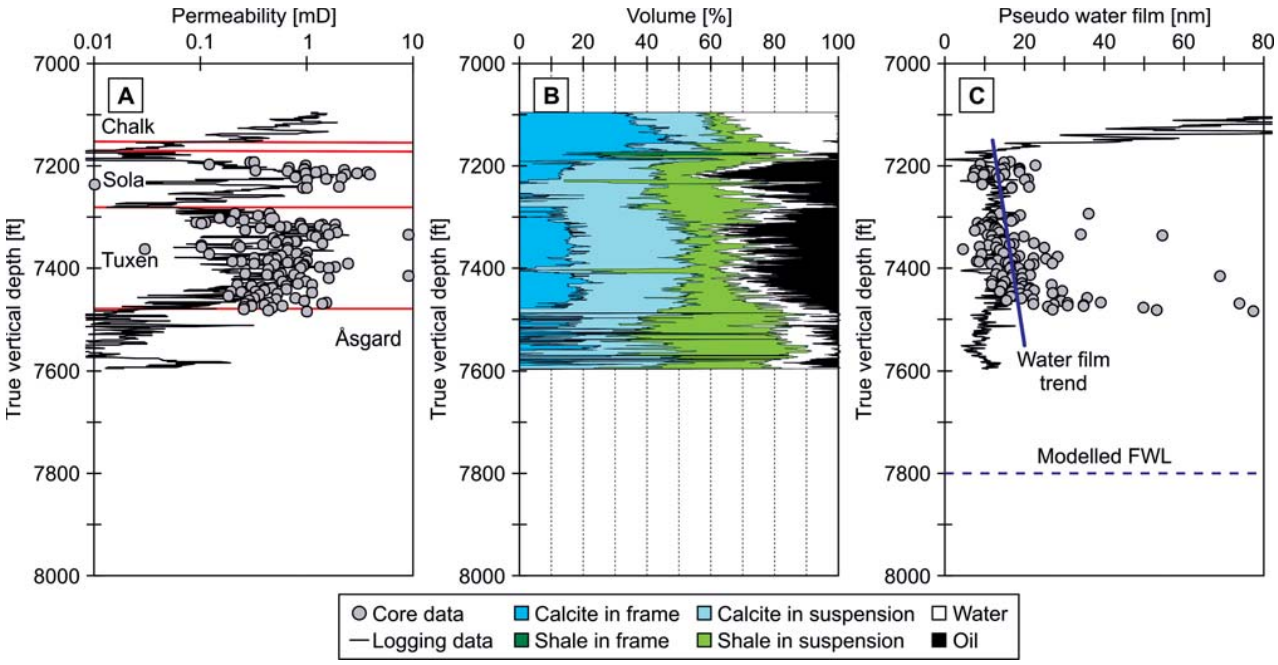


Fig. 10. Interpretation of core and logging data from Valdemar field. (A) Permeability from core analysis compared to permeability as calculated from density and natural gamma ray logs calibrated by core data. (B) Log of volumetric composition of the rock, based on petrophysical log interpretation and on iso-frame modeling. (C) Pseudo water film thickness is water saturation normalized to specific surface of pores. It is here calculated from core and from logging data. FWL is the free water level which may be estimated from the trend of the pseudo water film thickness (Larsen & Fabricius 2004). (Modified after Fabricius *et al*. 2005).

bearing intervals have relatively high porosity (Fig. 7, 8). As discussed above, the porosity-reduction may have been arrested at shallower burial as a consequence of the introduction of hydrocarbons (Fabricius *et al.* in press). When Terzaghi's law is used in its original form, the porosity covers a wide range for a given effective stress as a reflection of difference in texture. When Biot's coefficient is taken into account, the range narrows because wacke- and packstones tend to have higher β for a given porosity than mudstones (Fabricius *et al.* in press).

In the burial-stress interval dominated by mechanical compaction, the iso-frame value modeled from $v_P$ and $\rho_b$ is low and the estimated β consequently close to one, so that the two effective stress curves are similar (Fig. 7, 8). In the transition zone, the porosity reduction is arrested, whereas IF increases as a consequence of the pore-stiffening cementation. In the pure chalk of the Ontong Java Plateau, the transition zone begins at an effective stress of 4 MPa, in the silica rich Caribbean Site 999, the transition zone is met already at c. 2 MPa. The transition zone is easy to see when effective stress is calculated according to Terzaghi, but barely noticeable when β is taken into account. Subsequent pore-filling cementation is

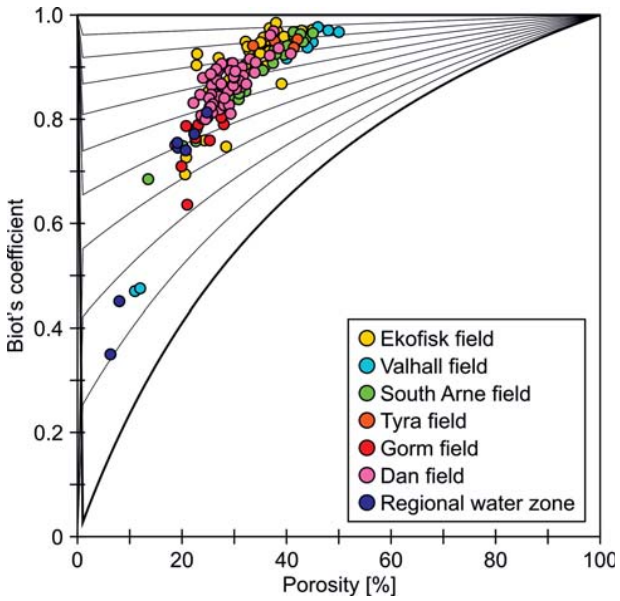


Fig. 11. Biot's coefficient versus porosity for North Sea field and water zone chalk samples with more than 90% carbonate. Iso-frame lines are shown in intervals of 0.1, ranging from 0 (uppermost) to 1 (lowest curve).

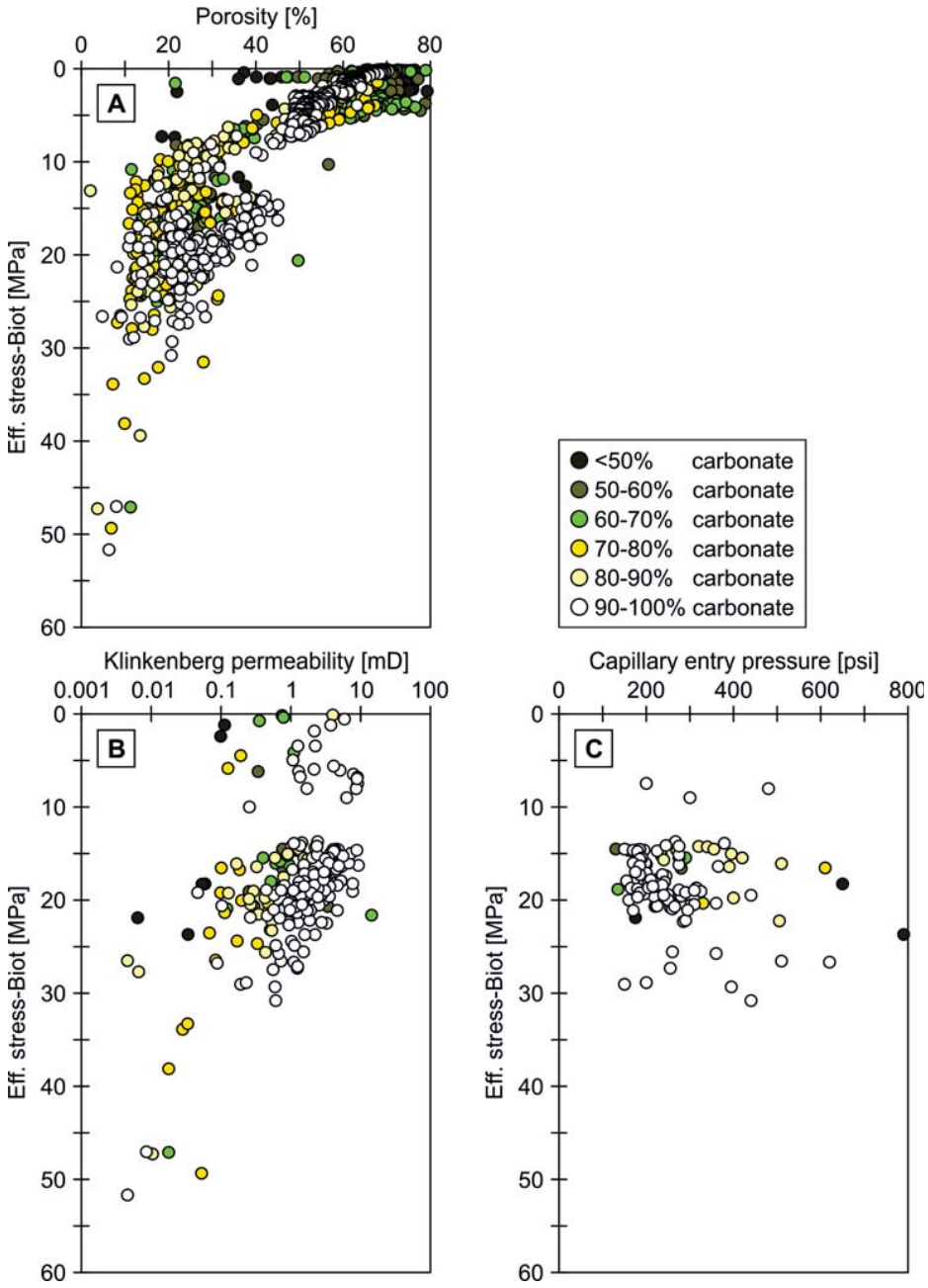


Fig. 12. Influence of carbonate content on effective stress trends of (A) porosity, (B) permeability and (C) capillary entry pressure. For the ODP-data Klinkenberg-permeability is modeled from porosity and specific surface (BET). For the remaining samples Klinkenberg permeability is calculated from gas permeability by using an empirical relationship (Mortensen *et al.* 1998).

reflected in a marked increase in IF and porosity reduction. The cementation front is easy to see from thermal maturation, TTI, and from effective stress according to Terzaghi.

The porosity reducing processes are thus best described when using TTI and Terzaghi's law, whereas the elastic properties of the resulting rock follows a simpler trend when taking β into account. During mechanical compaction, particle bridging cement, if present, is broken, and β is consequently 1. Similarly, stylolites are mechanically similar to open fractures because no cement bridges across the stylolite, so at the stylolite β is 1. By contrast, the chalk hosting the stylolite is cemented and β consequently lower than 1 indicating that it is under higher effective stress than the stylolite (Fabricius *et al.* in press).

## Chalk petrophysics

Basic petrophysical parameters describing the chalk as a reservoir for fluids are porosity, permeability and capillary entry pressure (Fig. 12). The permea-

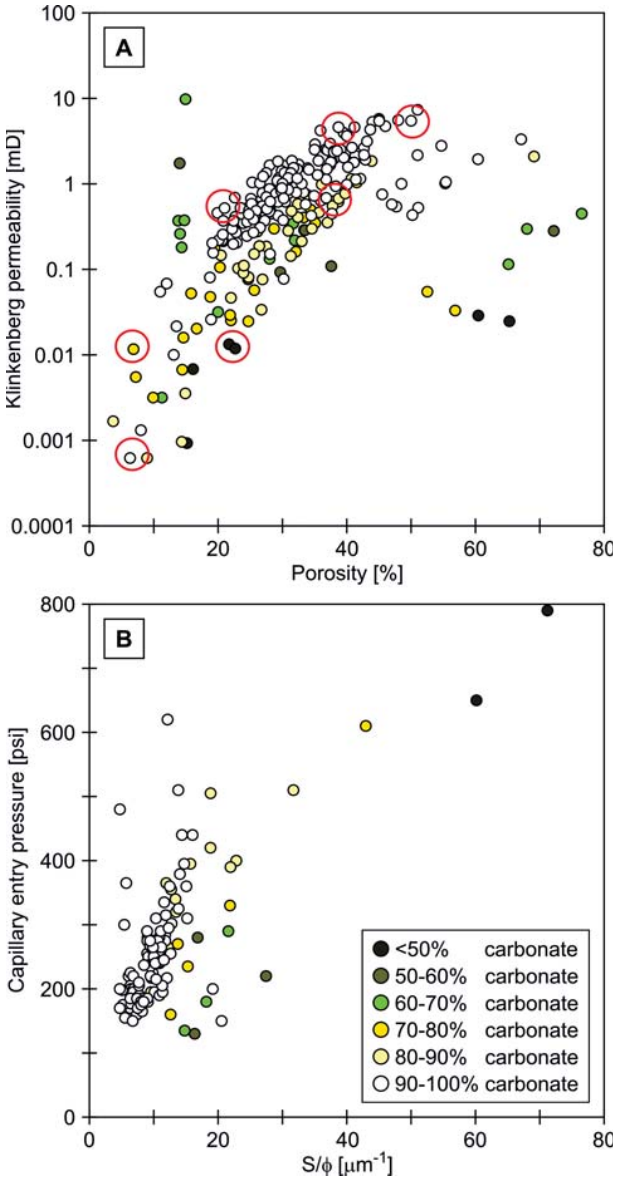


Fig. 13. Influence of carbonate content on porosity trends for (A) permeability and (B) equivalent inverse pore radius trend for capillary entry pressure. Red circles refer to images in Fig. 14. The inverse pore radius has been chosen for representation rather than the hydraulic radius, so that the linear relationship between $S/\phi$ and capillary entry pressure for pure carbonates becomes apparent. As evidenced from Fig. 12, the overall trend form high porosity and permeability to low values, reflects burial diagenesis.

bility describes the ability of a porous material to conduct fluid. It is here given as equivalent liquid permeability (Klinkenberg permeability, k) derived from gas permeability, $k_a$, by the empirical relationship of Mortensen *et al.* (1998):

$$k = 0.52\ k_a^{\ 1.083} \qquad (18)$$

where a permeability unit of mD is assumed (1 mD is close to $0.9869\ 10^{-15}$ m$^2$). The Klinkenberg permeability may also be derived experimentally by measuring gas permeability at a series of gas pressures. The Klinkenberg permeability is a property of the porous rock only and independent of liquid properties. The capillary entry pressure is the pressure required for a non-wetting fluid to enter a porous material saturated with a wetting fluid. It is here given for a mercury liquid-vapor system in the unit of psi (1 psi is close to 6.89 kPa). The capillary entry pressure may be re-calculated to a water-hydrocarbon system (Anderson 1987; Aguilera 2002). This is not done here due to the difference in pore water and hydrocarbons among the studied sites.

Porosity declines with increasing effective burial stress, and permeability also tends to do so at effective stress above 10 MPa. For a given effective stress, resulting porosity is correlated to composition of the solid phase. In the interval of mechanical compaction, mixed sediments among the studied samples tend to have higher porosity but lower permeability than the purer carbonate ooze (Fig. 12). Below the cementation front, depositional texture and carbonate content are reflected in porosity and permeability, so that poorly sorted chalk tends to have lower porosity and permeability for a given effective burial stress (Fig. 6, 12; Fabricius *et al.* 2007b). An unequivocal effective stress trend cannot be seen for capillary entry pressure among the studied samples (Fig. 12).

Porosity and permeability are related, but not simply so. Whereas depositional texture has significant influence on the porosity, the permeability is expected to be related to porosity and pore radius (or rather cross sectional pore area-sometimes referred to as pore throats) of the chalk (Fig. 13, 14). Capillary entry pressure is expected to be indirectly related to porosity, because it is controlled by the pore radius. Pore radius is most simply described in terms of porosity and specific surface, which are both easy to measure. Because porosity describes pore volume and specific surface describes pore surface, in combination they define pore radius in an ideal system. Specific surface is generally measured on dry powder and calculated from the adsorption isoterms for liquid nitrogen (Brunauer *et al.* 1938, thus the method is referred to as BET) and a reproducible value

may be obtained for dried chalk (Clausen & Fabricius 2000). The specific surface measured by BET, $S_{BET}$ is normally reported in area per solid mass or $m^2/g$, but for discussion of pore radius it must be normalized to bulk volume, because porosity and permeability both refer to bulk volume. The specific surface, S, becomes:

$$S = S_{BET}\, \rho_{calcite}\, (1-\phi) \tag{19}$$

And the equivalent hydraulic radius becomes:

$$\phi / S \tag{20}$$

In tubular parallel pores, hydraulic radius then becomes half the pore radius. We consequently find a positive relationship between capillary entry pressure and $S/\phi$ for pure chalk, whereas chalk with a significant content of silica and silicates for a given porosity has a relatively high capillary entry pressure as a reflection of relatively low homogeneity (Fig. 13; Røgen & Fabricius 2002).

In accordance with Kozeny (1927) the permeability may be expressed:

$$k = c\, \phi\, (\phi/S)^2 = c\, \phi^3/S^2 \tag{21}$$

Mortensen *et al.* (1998) modeled c as a function of $\phi$ by deriving an equation for permeability in orthogonal penetrating tubes allowing flow in three directions, but where only flow in the direction of the overall pressure gradient is taken into account. Pressure equilibration in directions perpendicular to the pressure gradient is thus assumed instantaneous. For circular tubes Mortensen *et al.* (1998) obtained:

$$c = \left( 4 \cos\left( \frac{1}{3} \arccos\left( \phi \frac{8^2}{\pi^3} - 1 \right) + \frac{4}{3}\pi \right) + 4 \right)^{-1} \tag{22}$$

Equation 22 predicts c of 0.21 at 20% porosity and c of 0.27 at 60% porosity. The advantage of the model is that it avoids a concept of hypothetical winding pores, which matches poorly with petrography. By using this model Mortensen *et al.* (1998) found that k for chalk may be predicted from Kozenys equation without introducing empirical factors. This must be a consequence of the relatively high homogeneity of chalk at the scale where permeability is measured in the laboratory. So in spite of large textural variations, chalk is surprisingly homogeneous with respect to petrophysical properties –probably a consequence of relatively uniform size and smoothness of the single calcite crystals in a given sample.

Permeability and capillary entry pressure are largely controlled by porosity and specific surface and we find accordingly that samples with less than 90% carbonate tend to have relatively low permeability as a reflection of larger specific surface of the silicates (Fig. 13, 14; Røgen & Fabricius 2002), and that for a given porosity samples with 80-90% carbonate have higher capillary entry pressure than purer chalk (Fig. 13; Røgen & Fabricius 2002). At effective stress up to 10 MPa, permeability apparently hardly decreases and may even have a tendency to increase, in spite of the falling porosity (Fig. 12). The permeability from this stress-interval was calculated from Equation 21, so the apparent tendency reflects the dropping specific surface as the chalk re-crystallizes. With respect to texture, it appears that samples with sorted matrix, but a wackestone microtexture tend to have high permeability for a given porosity, whereas samples with low permeability for a given porosity, tend to have mudstone texture, but a poorly sorted matrix (Fig. 13). It should be borne in mind, that fractured chalk is not homogeneous at the scale of permeability measurement and will tend to have relatively high permeability. It is also noteworthy that although stylolites mechanically act as fractures, stylolites as they are typically found in reservoir chalk probably only have significant positive influence on permeability when they are associated with open fractures (Lind *et al.* 1994). A negative influence on permeability perpendicular to stylolites where the clay drape is a relatively thick is conceptually logical and has been inferred by several authors (*e.g.* Safaricz & Davison 2005).

The reservoir quality of North Sea chalk varies among fields and formations, as illustrated by permeability-porosity cross plots (Fig. 15; Fabricius *et al.* 2007b). The Tor Formation samples tend to have higher porosity, and for a given porosity to have higher permeability than the samples from Ekofisk Formation, and among the samples from Tor Formation, samples from Gorm field tend to have highest permeability for a given porosity, whereas samples from South Arne field tend to have lowest permeability (Fig. 15). This difference in reservoir properties is reflected in the specific surface (Fig. 16). By comparing the specific surface of a sample to the specific surface of the non-carbonate fraction (insoluble residue) we find that for the regional water zone samples, the carbonate have close to zero contribution to $S_{BET}$. This is probably due to the high degree of pore-filling calcite-cementation in the water zone, which causes the calcite phase to have small specific surface. The relatively high $S_{BET}$ of these samples is caused by the content of smectite-chlorite (refer Fig. 6). The samples from Dan and Gorm are mainly from the Tor Formation. The carbonate phase contributes

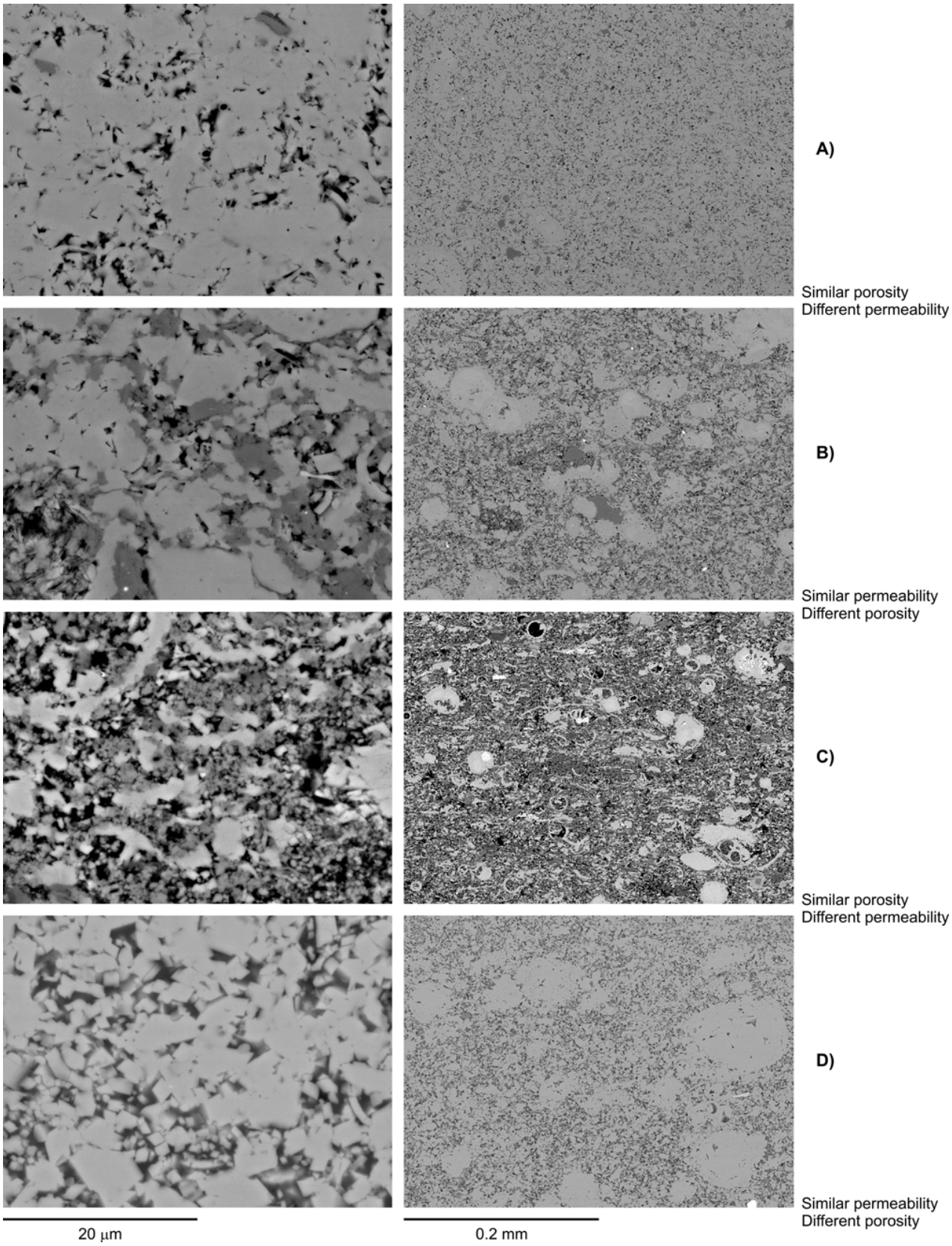
A)
Similar porosity
Different permeability
B)
Similar permeability
Different porosity
C)
Similar porosity
Different permeability
D)
Similar permeability
Different porosity
20 μm
0.2 mm

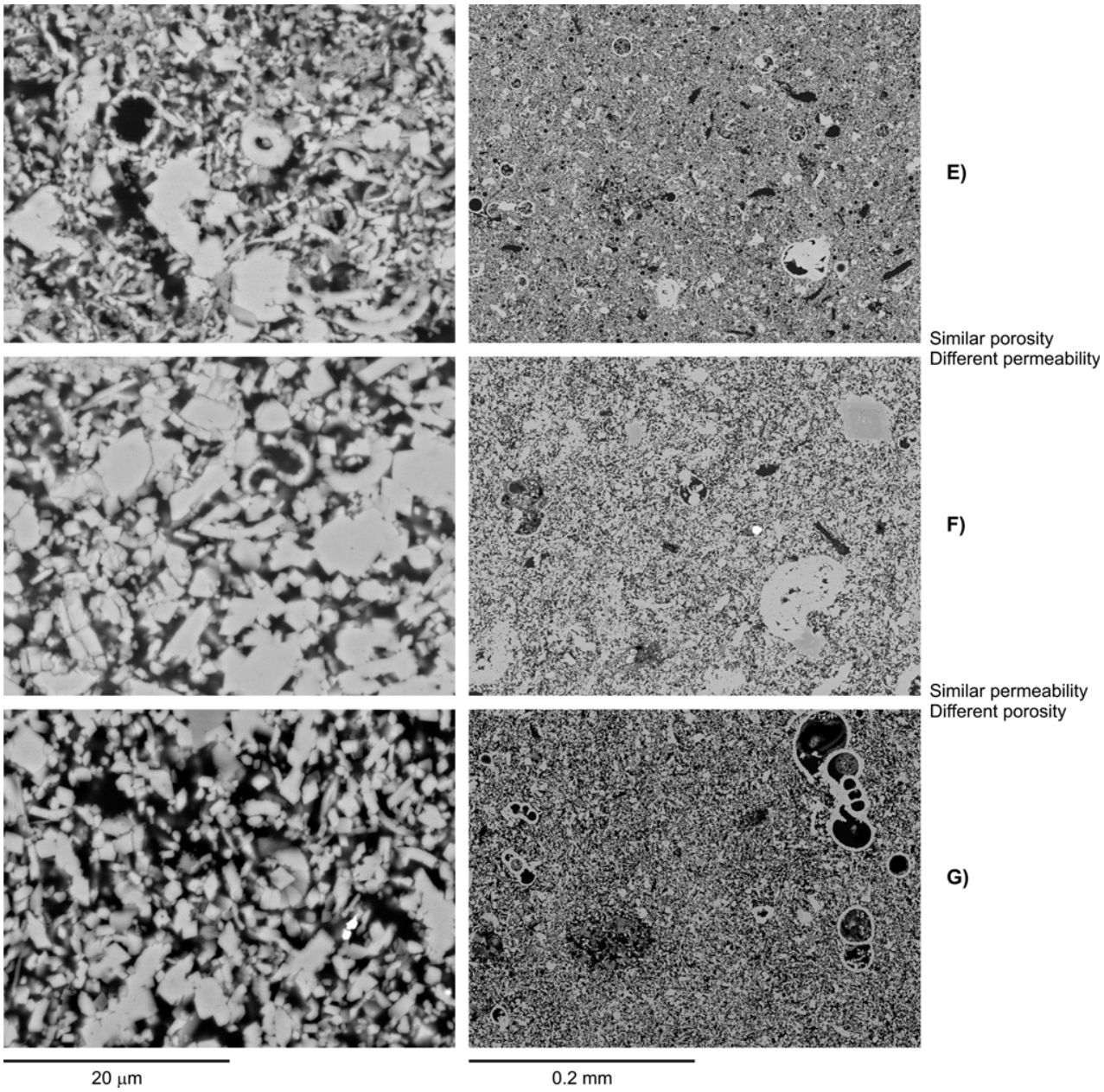


Fig. 14. Backscatter electron micrographs of polished North Sea chalk at two magnifications illustrating textural control on porosity and permeability. (A) Sample with mudstone texture from the water zone in the Hod Formation of the well West Lulu-1. Depth 3361 m tvd. The sample contains 93% carbonate, porosity is 6.3% and Klinkenberg permeability is 0.0006 mD. Biot's coefficient is 0.35. (B) Sample with wackestone texture from the water zone in the Hidra Formation of the well Gert-1. Depth 3877 m tvd. The sample contains 74% carbonate as well as probably authigenic quartz crystals (grey). The carbonate cement filling microfossils contains a small concentration of Fe and thus has a lighter grey color. Porosity is 6.9% and Klinkenberg permeability is 0.012 mD. Biot's coefficient is 0.53. (C) Sample with laminated mudstone/wackestone texture from the Ekofisk Formation of the Ekofisk field, well 2/4 K4. Depth 3062 m tvd. The sample contains 49.8% carbonate plus a substantial amount of submicron-size quartz (grey), porosity is 21.7% and Klinkenberg permeability is 0.013 mD. Biot's coefficient is 0.92. Wite crystals are pyrite. (D) Sample with wackestone texture from the Tor Formation of the Gorm field, well N-22X. Depth 2186 m tvd. The sample contains 98% carbonate, microfossils are cemented, porosity is 21% and Klinkenberg permeability is 0.52 mD. Biot's coefficient is 0.64. (E) Sample with mudstone texture from the Ekofisk Formation of the Tyra field, well E-5X. Depth 2025 m tvd. The sample contains 85% carbonate, porosity is 38% and Klinkenberg permeability is 0.55 mD. Biot's coefficient is 0.93. Molds after probably siliceous fossils are widespread as black holes in the low magnification image, whereas submicron size quartz particles are visible in the high magnification image. Microfossils are partly calcite-cemented. (F) Sample with wackestone texture from the Ekofisk Formation of the Ekofisk field, well 2/4-K4. Depth 3038 m tvd. The sample contains 97% carbonate, porosity is 40% and Klinkenberg permeability is 4.0 mD. Biot's coefficient is 0.96. Dolomite is visible as grey rhombs, and moldic porosity is noted as single black holes in the low magnification image. Single submicron size quartz particles are visible on the high magnification image. (G). Sample with mudstone texture from the Tor Formation of the Valhall field, well 2/8-A2. Depth 2473 m tvd. The sample contains 97% carbonate, porosity is 50% and Klinkenberg permeability is 5.5 mD. Biot's coefficient is 0.97. Calcareous microfossils have maintained intra-fossil porosity, whereas siliceous microfossils (dark grey) are poorly preserved.

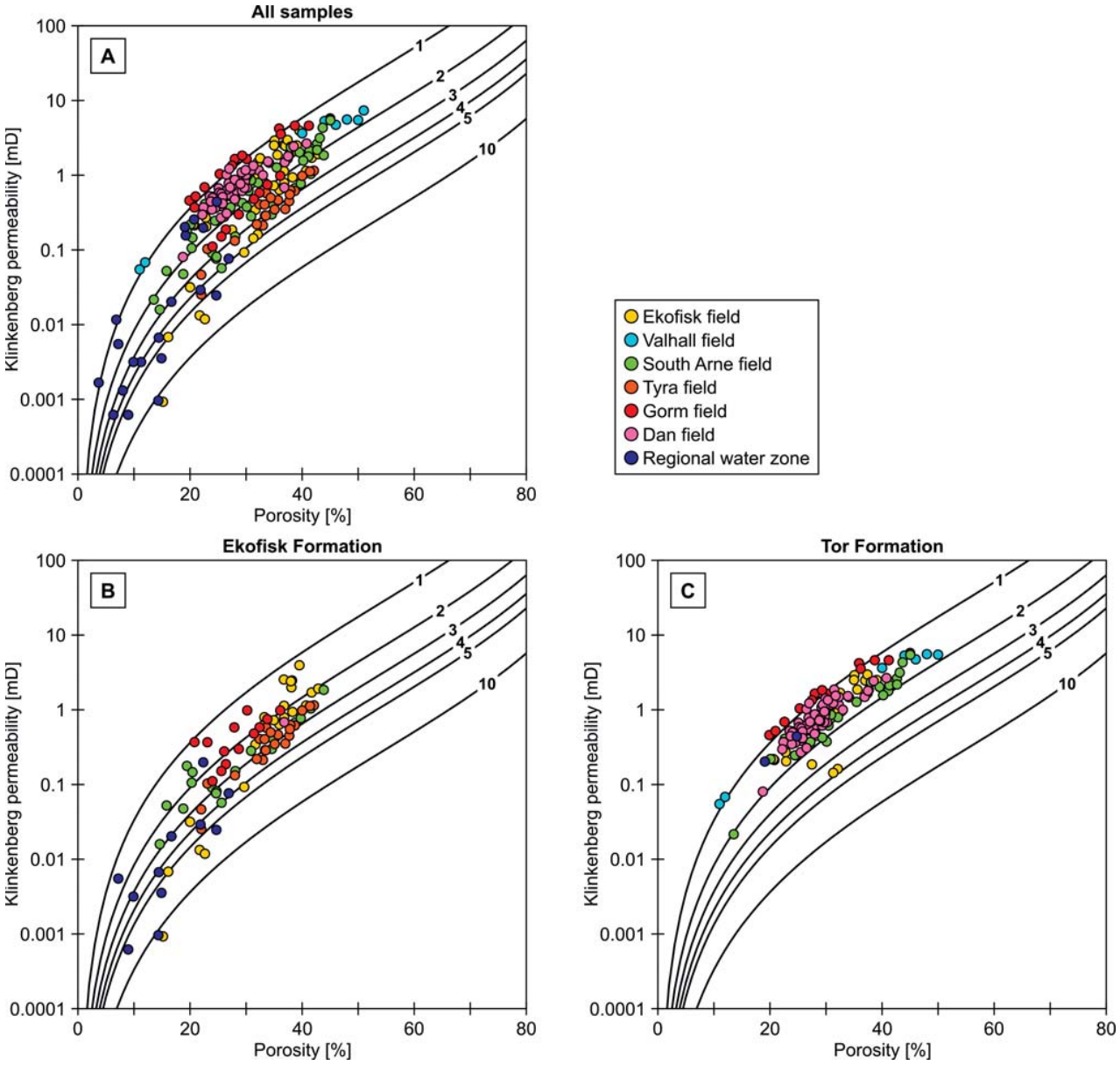


Fig. 15. Permeability vs. porosity for all samples (A) and as split into formations (B, C). Permeability - porosity trends vary among the chalk fields for Tor Formation samples, whereas the samples from Ekofisk Formation are more scattered and do not show a similar pattern. The curves represent equal BET in $m^2/g$ as calculated by using Kozeny's equation. BET refers to specific surface as measured by nitrogen adsorption. It tends to be higher in chalk from Ekofisk Formation than chalk from Tor Formation.

around 0.9 $m^2/g$ to $S_{BET}$, whereas a modest smectite content may give up to the same contribution to $S_{BET}$ for the Dan field samples where capillary entry pressure is directly predictable (Fig. 16).

Samples from the Ekofisk field generally follow the trend of the Dan field, although they are more scattered as a reflection of including samples from both Ekofisk and Tor formations. The Tyra field samples are from the Ekofisk Formation and several are poorly sorted as indicated by a relatively low capillary entry pressure (Fig. 16). The carbonate phase contributes around 2 $m^2/g$ to $S_{BET}$ as an indication of relatively low degree of recrystallization. Quartz, kaolinite and smectite contribute up to the same amount. For samples from South Arne field, the contribution to $S_{BET}$ by the carbonate phase varies between 0.1 and 2.2 $m^2/g$ as a reflection of including samples from both Tor and Ekofisk Formation, but the pure carbonate samples indicate that not only a relatively high content of silica and kaolinite but also a small crystal size of the calcite contributes to the overall relative low permeability of South Arne chalk

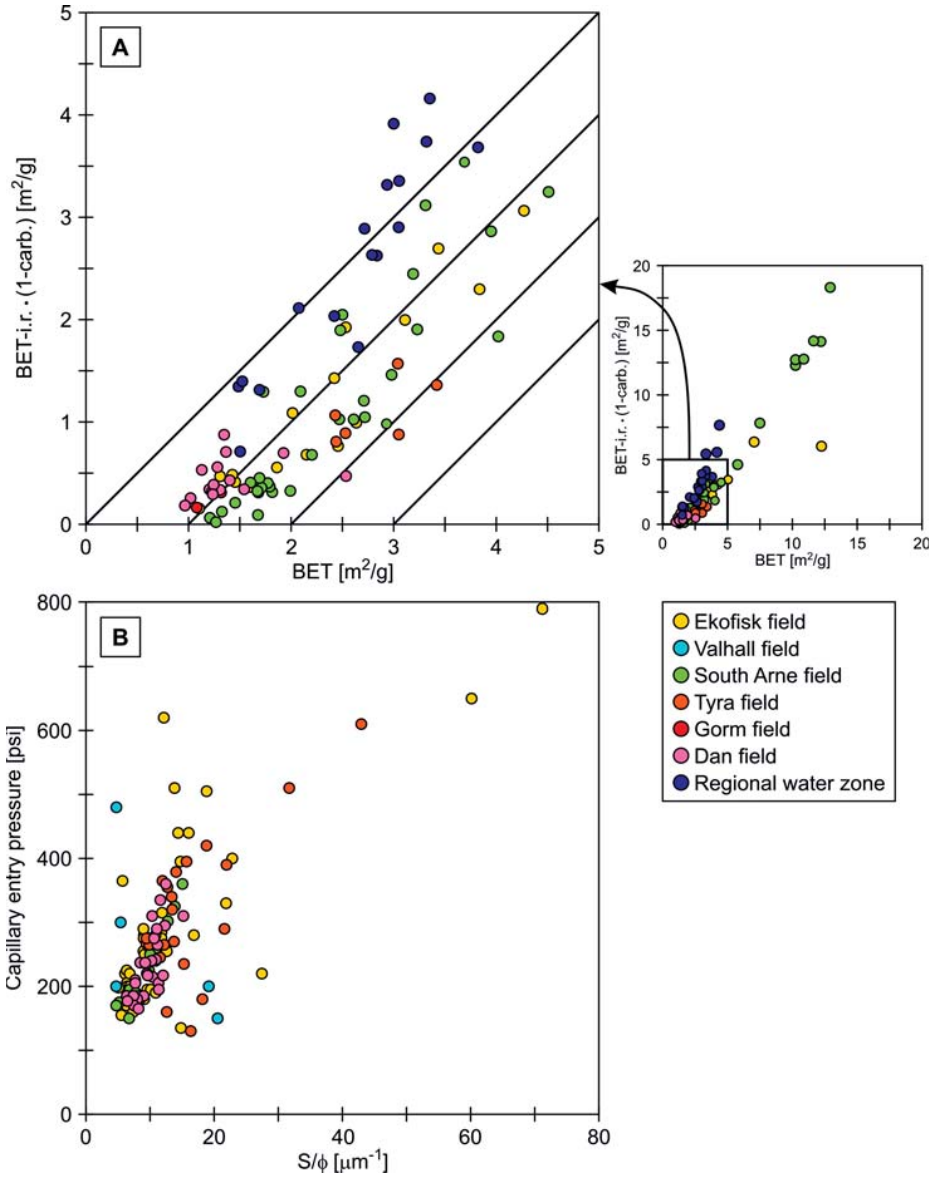


Fig. 16. (A) Regional variation in specific surface of total sample (BET) as compared to specific surface of non-carbonate fraction (BET-i. r.) normalized to total sample; and (B) regional variation in capillary pressure vs. equivalent pore radius, S/ϕ. We find that the specific surface is partially related to the calcite surface, partially to the non-calcite surface (mainly silica). The distribution varies regionally. Whereas BET of the water zone samples is mainly due to non-carbonates, BET of samples from South Arne and Tyra is more influenced by the calcite surface. (Tyra, but not South Arne is only represented by samples from Ekofisk Formation). In spite of the high non-carbonate influence on specific surface, samples from South Arne field follows the "pure carbonate trend" in the capillary entry pressure S/ϕ plot (refer Fig. 13).

(Fig. 15, 16). Because the effect is not related to stratigraphy, it is hardly due to an original smaller crystal size in the chalk-forming fossils or a more intense mechanical breakdown by deposit feeders. The relatively small calcite crystal size in South Arne chalk is thus probably a reflection of the lack of pore filling cementation (overgrowth), indicating that although the pore-stiffening cementation causes South Arne chalk to have high elastic moduli for a given porosity, the high porosity is not fully reflected in a higher permeability.

# Conclusion

## Reservoir quality of chalk matrix

Porosity of newly deposited calcareous ooze of chalk facies is high, around 70%. Before the chalk reaches the cementation front at an effective stress of 5–10 MPa, chalk porosity is mainly controlled by the degree of mechanical compaction. This process will vane as recrystallization causes formation of contact cement and the chalk stiffens. At sufficient effective stress, pressure solution of stylolites adds Ca and carbonate ions to the pore water and pore-filling cementation may set in. After the onset of pore-filling cementation, overall porosity drops, but the deposi-

tional texture of the chalk will have a large influence on chalk porosity because microfossils tend to become completely filled by cement. Chalk mudstones thus tend to be more porous than wackestones or packstones. The picture is complicated because the sorting of the mud-matrix also plays a role, so that silicate rich chalk tends to have low porosity. Re-deposited, clast bearing chalk may have high or low porosity depending on the microtexture and sorting of mud-matrix.

In hydrocarbon-bearing chalk, depth-wise porosity reduction tends to be arrested, so that porosity remains high for a given burial. This may be due to hydrocarbon-adsorption to the silicates of stylolites, which will prevent pressure dissolution and thus close the local source of Ca and carbonate ions. Under these conditions cementation requires diffusion from the water zone. This process may be slow, because the diffusion has to take place in the thin water film coating the pore surface in the hydrocarbon zone. In the absence of stylolites, it may be inferred that porosity can remain high during burial, even where no hydrocarbons are present.

Permeability and capillary entry pressure of chalk is controlled by porosity and the specific surface of the chalk. The specific surface is primarily due to the content of fine grained silica and clay, especially in cemented chalk. In chalk where degree of recrystallization is relatively low, the specific surface of the calcite plays a significant role.

# Interpretation of elastic moduli

Upper bounds for the static elastic moduli of the chalk may be predicted directly from dynamic moduli calculated from the sonic velocity and density.

Iso-frame modeling of elastic moduli allows quantification of the degree of pore-stiffening cementation. The model implies that for chalk with similar iso-frame value, porosity variation is controlled by sorting as reflected in silicate content and depositional texture. For chalk with similar porosity, variation in iso-frame value implies pore-stiffening cementation. The process of pore-filling cementation will cause porosity to decrease and iso-frame value to increase.

Biot's coefficient may be calculated from elastic moduli, and if only one modulus is available, by iso-frame modeling. Biot's coefficient indicates to which extent pore pressure in a given sedimentary rock in a sedimentary basin counteracts the stress from the overburden.

## Deformation of chalk

Mechanical compaction and pressure dissolution is controlled by the effective stress defined according to Terzaghis law by assuming Biot's coefficient equal to one. This is because mechanical compaction involves breaking of possible grain contacts, and because stylolites are mechanically similar to fractures.

Elastic deformation of the chalk upon burial must be calculated from the effective stress by taking Biot's coefficient into account, because the contact cement and pore filling cement bind the calcite particles together. The effective stress in the chalk between stylolites is thus higher than at the stylolites.

Water weakening of chalk has been explained in several ways. It may occur because in a polar medium less energy is required to neutralize the electrical charges on calcite surfaces exposed by breakage of contact cement or calcite crystals. In a dry or oil saturated chalk the water film bridging the contact cement thus gets a high shear strength, possibly also reflected in a relatively high shear modulus of dry chalk.

## Controls on chalk diagenesis

Diagenesis of the chalk follows different trends depending on rate of deposition and content of organic mater. Where deposition is intermittent, microbial action dominates, and carbonate or apatite-cemented hardgrounds form. Where organic matter is relatively abundant concretions of pyrite and barite may form by microbial action. Where the sediment is rich in opal, chert nodules may also form at this stage, possibly helped by microbial action.

Where deposition is continuous and content of organic matter is sparse, microbial action vanes after removal of the organic matter of the carbonate ooze, and pyrite and barite are generally found as dispersed crystals rather than concretions. Subsequent diagenesis probably takes place in equilibrium with the pore water as controlled by time, increasing temperature, and increasing burial stress. The main action of pore pressure is to counteract the stress from overlying sediments.

## Silica and chert

The burial diagenesis involves recrystallization of the calcite; gradual time- and temperature controlled transformation of silica from opal-A to opal CT to quartz; and transformation of clay minerals. The silica transformation involves dissolution of opal-A and

re-precipitation of opal-CT which is transformed to quartz. The diagenetic quartz will appear as submicron-size dispersed crystallites or where silica is a dominating constituent as chert. In spite of a relatively high silica content chert may be rarer and dispersed silica more common in chalk dominated by burial diagenesis as opposed to chalk dominated by early bacterial action.

### Clay minerals and stylolites

The clay mineralogy varies regionally and with depth indicating differences in provenance probably combined with a depth-wise diagenetic transition from smectite to mixed smectite-illite, and further to smectite-chlorite.

The transformation of clay minerals involves re-precipitation and the formation of flaser structures or where clay is more localized formation of stylolites. These structures form the target for pressure dissolution at sufficient effective stress (above 3–5 MPa). By this process calcite is dissolved and may re-precipitate.

The re-precipitation of calcite is influenced by the silica diagenesis. Where opal is a major constituent and the pore water is rich in silica, Ca- silica complexes may form and retard pore-filling calcite cementation. The course of action depends on the content of silica, temperature and age of the chalk, when pressure dissolution begins. The onset of calcite cementation may be seen as a cementation front drastically reducing chalk porosity.

## Acknowledgements

This paper builds on work done by several Ph.D. students, master students, and technicians. It also benefits from contributions from co-authors, collaborators and discussion partners. Financial support from outside DTU is acknowledged from The Danish Energy Research Program, The Joint Chalk Research Program, The Nordic Energy Research Program, Mærsk Olie og Gas AS, Amerada Hess A/S, DONG A/S, Denerco oil A/S, The Ocean Drilling Program and Danish Natural Science Foundation. Samples for study were obtained from The Ocean Drilling Program, Mærsk Olie og Gas AS, GEUS, Amerada Hess A/S, Amoco-BP, and Conoco-Philips.

Among Ph.D students thanks are primarily due to Mai Borre, Liselotte Clausen, Lars Gommesen, Morten Leth Hjuler, Jens Martin Hvid, Jens Keld Larsen, Lene Madsen, Casper Olsen, and Birte Røgen.

Among master students special thanks are due to Md. Monzurul Alam, Azher Bilal, Abdelhakim Chtioui, Amin Dejkam, Frederik Ditlevsen, Peter Grøn, Kathrine Hedegaard, Anton Henriksen, Kathrine Jørgensen, Heidi Olsen, Jeanette Mortensen, Jennifer Lee Moss, Wasim Nasir, Md. Asfaq Rana, Christina Rasmussen, Eivind Henze Samuelsen, Anja Theresa Theilgaard, and Julie Bjerring Zandbergen.

Among technicians at DTU special thanks are due to Hector Ampuero Diaz, Kirsten Hvid Carlsen, Mimi Christensen, Torben Dolin, Bente Frydenlund, Vibeke Knudsen, Helge Kragh, Laila Leth, Sinh Hy Nguyen, Alexandra Claudius Nielsen, and Inger Søndergaard.

Among colleagues and collaborators I whish to direct special thanks to Peter Japsen, Peter Frykman, Finn Engstrøm, Aubrey Ford, Bent Hansen, Niels Foged, Wolfgang Berger and Gary Mavko.

Peter Frykman and an anonymous reviewer gave constructive comments to a previous version of this paper.

## Dansk sammendrag

Skrivekridt består af biogen calcit med et varierende tilskud af biogen kisel i form af opal-A, som dog ofte er opløst og erstattet af mikrokrystallin opal-CT eller dets omdannelsprodukt mikrokrystallin kvarts. Dertil kommer mindre bidrag af erosionsprodukter som siltkorn af kvarts eller feldspat og ler. Vulkansk aske kan også forekomme og vil sammen med feldspat og det detritale ler danne udgangspunkt for nydannelse af ler efterhånden som sedimentet begraves under yngre aflejringer. Som udgangspunkt er det nyaflejrede kalkslam højporøst, men herefter afgøres sedimentets skæbne af om det er udsat for forholdsvis hurtig begravelse eller om det er aflejret på forholdsvis lavt vand, eller hvor der af andre grunde kun sker lejlighedsvis aflejring. Ligger kalkslammet hen uden at blive dækket af nye lag, kan mikroorganismer forårsage udfældninger af karbonater og fosfater så havbunden bliver lavporøs og hård. Hvis kalkslammet er forholdsvis rigt på organisk materiale kan mikroorganismer forårsage dannelse af konkretioner af pyrit eller af kisel i form af flint. Er kalkslammet derimod fattigt på organisk materiale, som det typisk er tilfældet langt fra kysten vil mikroorganismerne kunne danne finfordelt pyrit, mens kiselen begraves som opal-A, der efterhånden opløses og erstattes af opal-CT der typisk vil udfælde som fine partikler i porer og sprækker. Hvor sedimentet som udgangspunkt var rigt på opal, eller hvor opalen er blevet koncentreret i sprækker, kan der dan-

nes flintlag. Lermineraler vil også kunne opløses og genudfældes som mikrostylolit-zoner (flaser-strukturer) eller stylolitkim.

Det porøse kalkslam vil efterhånden blive kompakteret af vægten af de overliggende sedimenter, mens de enkelte calcitkrystaller kommer i ligevægt med porevandet og gradvis mister deres biogene facon. Vægten af de overliggende sedimenter og vand udsætter kalkslammet for en totalspænding, men det er den effektive spænding, d.v.s totalspændingen minus trykket i porevandet, der afgør hvor meget kalkslammet kompakteres mekanisk. Denne proces fortsætter typisk til kalkens porøsitet er faldet til 40–50%. Hvis begravelsen sker langsomt nok, kan kalkkornene danne kontaktcement via reaktion med porevandet, og en høj porøsitet kan bevares. I kontaktcementen mødes krystaller fra to nabokorn, som bindes sammen af en vandfilm. Øges den effektive spænding ved en senere lejlighed, vil kompaktionen kunne genoptages, men det kræver at vandfilmen brydes – en proces som kræver større stress jo mindre polær porevæsken er.

Når den mekaniske kompaktion er klinget af afhænger den videre udvikling af tilstedeværelsen af stylolitkim, for når den effektive spænding bliver høj nok kan der her ske trykopløsning af calciten, hvor den presses ned mod lermineralernes elektriske dobbeltlag, som kan lede Ca-ioner. Porevandet tilføres altså herved Ca-ioner og ofte vil stylolitdannelsen derfor gøre at kalkens porer fyldes mere eller mindre op med calcit cement. Hvis kislen endnu ikke er omdannet til kvarts, kan porevandets indhold af silicium være forholdvis højt og udfældningen af calcit kan forsinkes på grund af dannelsen af Ca-silikatkomplekser i porevandet. Mangler stylolitkim i form af lermineraler, må det forventes at kalken kan bevare høj porøsitet til dybere begravelse end normalt.

Flere af kalkens andre fysiske egenskaber er primært betinget af kalkens porøsitet. For eksempel vil kalkens elasticitet afhænge af porøsiteten, men også af hvor effektivt kalkkornene er cementeret sammen. Kalkens permeabilitet for væske er også primært afhængig af porøsiteten, men her har arealet af kontaktfladen mellem fast fase og porer også betydning. Dette areal beskrives som den specifikke overflade, hvor permeabiliteten falder med stigende specifik overflade. Dens størrelse afhænger primært af kalkens indhold af finfordelt kisel og ler, men også i nogen grad af kalkkrystallernes størrelse. I cm-skala er kalken så homogen at permeabiliteten kan modelleres direkte uden brug af korrektionsfaktorer. Porøsiteten og den specifikke overflade afgør også det kapillære tærskeltryk. Her kan tærskeltrykket kun forudsiges empirisk og kun for den reneste kalk. Kalkens elastiske egenskaber kan modelleres ved hjælp af effektiv medium-teori ud fra elastiske moduli beregnet ud fra lydhastighed og densitet. Tages porøsiteten i betragtning kan de øvrige elastiske moduli forudsiges ud fra en enkelt modulus, og det er muligt at forudsige, hvordan moduli ændres med ændret porevæske. Modellering af elastiske moduli gør det muligt at definere en faktor, der beskriver kalkens grad af cementering.

# References


Aguilera, R. 2002: Incorporating capillary pressure, pore throat aperture radii, height above free-water table, and Winland $r_{35}$ values on Pickett plots. AAPG Bulletin, 86, 605-624.

Andersen, M.A. 1995: Petroleum Research in Chalk. Joint Chalk Research Phase IV, Rogaland Research, Stavanger, Norway, 0-179.

Anderson, J.K. 1999: The capabilities and challenges of the seismic method in chalk exploration. In: Fleet, A.J. & Boldy, S.A.R. (eds): Petroleum Geology of North West Europe, Proceedings of the 5th conference. Geological Society London, 939-947.

Anderson, W.G. 1987: Wettability literature survey- Part 4: Effects of wettability on capillary pressure. Journal of Petroleum Technology 39, 1283-1300.

Andrews, J. E., Packham, G. *et al.* 1975. Initial Reports of the Deep Sea Drilling Project, 30, Washington (U.S. Government Printing Office), 1-753.

Anselmeti, F.S. & Eberli, G.P. 2001: Sonic velocity in carbonates –A combined product of depositional lithology and diagenetic alterations. In: Ginsburg, R.N. (ed.): Subsurface Geology of a Prograding Carbonate Platform Margin, Great Bahama Bank: Results of the Bahamas Drilling Project: SEPM Special Publication 70, 193-216.

Audet, D.M. 1995: Modelling of porosity evolution and mechanical compaction of calcareous sediment. Sedimentology 42, 355-373.

Baker, P.A., Gieskes, J.M. & Eldersfield, H. 1982: Diagenesis of carbonates in deep-sea sediments – evidence from Sr/Ca ratios and interstitial dissolved $Sr^{2+}$ data. Journal of Sedimentary Petrology 52, 71-82.

Berger, W.H. 1973: Deep-Sea carbonates – evidence for a coccolith lysocline. Deep-Sea Research 20, 917-921.

Berger, W.H. & Johnson, T.C. 1976: Deep-sea carbonates: dissolution and mass wasting on Ontong- Java Plateau. Science 192, 785-787.

Berger, W.H. & Lind I.L. 1997: Abundance of color bands in Neogene carbonate sediments on Ontong Java Plateau: a proxy for sedimentation rate? Marine Geology 144, 1-8.

Berger, W.H. & Winterer, E.L. 1974: Plate stratigraphy and the fluctuating carbonate line. In: Hsü, K. & Jenkyns, H.C. (eds.): Pelagic sediments: on land and under the sea. Special Publication of the International Association of Sedimentologists 1, 11-48.

Berner, R.A. 1975: The role of magnesium in the crystal growth of calcite and aragonite from sea water. Geochimica et Cosmochimica Acta 39, 489-504.

Berryman, J.G., 1980: Long-wavelength propagation in com-

posite elastic media II. Ellipsoidal inclusions: Journal of the Acoustic Society of America 68, 1820-1831.
Biot, M.A. & Willis, D.G. 1957: The elastic coefficients of the theory of consolidation. Journal of Applied Mechanics, December. 594-601.
Borre, M. 1997: Porosity variation in Cenozoic and Upper Cretaceous Chalk from the Ontong Java Plateau – a discussion of image analysis data. In Middleton, M. F. (ed.) Research in Petroleum Technology. Nordic Petroleum Series 3, Ås Norway, 1-15.
Borre, M. 1998: Ultrasonic velocity of North Sea Chalk –predicting saturated data from dry. In Middleton, M. F. (ed.) Research in Petroleum Technology. Nordic Petroleum Series 4, Ås Norway, 71-98.
Borre, M.K. & Fabricius (Lind), I.L. 1998: Chemical and mechanical processes during burial diagenesis of chalk: an interpretation based on specific surface data of deep-sea sediments. Sedimentology 45, 755-769.
Borre, M.K. & Fabricius, I.L. 1999: Chalk texture in the North Sea and the Ontong Java Plateau (abstract) 19th Reginal Meeting of Sedimentology, Copenhagen, University of Copenhagen, p. 41.
Borre, M.K. & Fabricius, I.L. 2001: Ultrasonic velocities of water saturated chalk from the Gorm field, Danish North Sea: sensitivity to stress and applicability of Gassmann's equation. In Fabricius, I. L. (ed.) Nordic Petroleum Series V: Research in Petroleum Technology, 1-18, Nordisk Energiforskning.
Borre, M., Lind, I. & Mortensen, J. 1997: Specific surface as a measure of burial diagenesis of chalk. Zentralblatt für Geolologie und Paläontologie Teil 1 1995, 1071-1078.
Borre, M., Beales, V., Frank, S., Eiane, T., Gravem, T. & Eikenes, S. 2004: Fluid substitution in horizontal chalk wells and the effect on acoustic rock propeperties. A case study comparing logging while drilling and wireline acoustic data. SPWLA 45th Annual Logging Symposium, June 6-9, 2004.
Brewster, J., Dangerfield, J. & Farrell, H. 1986: The geology and geophysics of the Ekofisk field waterflood. Marine and Petroleum Geology, 3, 139-169.
Bromley, R.G. 1967: Some observations on burrows of thalassinidean Crustacea in chalk hardgrounds. Quaternary Journal of the Geological Society of London 123, 157-182.
Brunauer, S., Emmett, P.H. & Teller, E. 1938: Adsorption of gases in multimolecular layers. Journal of the American Chemical Society 60, 309-319.
Bürki, P.M., Dent Glasser, L.S. & Smith, D.N. 1982: Surface coatings on ancient coccoliths. Nature 297, 145-147.
Calvert, S.E. 1974: Deposition and diagenesis of silica in marine sediments. In: Hsü, K.J. & Jenkyns, H.C. (eds): Pelagic Sediments on Land and Under the Sea. Special Publication of the International Association of Sedimentologists 1, 273-299.
Castagna, J.P., Batzle, M.L. & Kan, T.K. 1993: Rock physics – the link between rock properties and AVO response in offset-reflectivity –Theory and practice of AVO analysis. In Castagna, J. P. & Bachus, M. eds. Investigations in Geophysics 8, SEG, Tulsa Oklahoma, 135-171.
Clausen, L. & Fabricius, I. 2000: BET measurements: outgassing of Minerals. Journal of Colloid and Interface Science 227, 7-15.
Clausen, L., Fabricius, I. & Madsen, L. 2001: Adsorption of pesticides onto quartz, calcite, kaolinite, and a-alumina. Journal of Environmental Quality 30, 846-857.
Clayton, C.J. 1986: The chemical environment of flint formation in Upper Cretaceous chalks: In Sieveking, G. de G. & Hart, M. B. eds. The Scientific Study of Flint and Chert, Cambridge University Press, NY, 45-54.
Crabtree, B., Fritsen, A., Mandzuich, K., Moe, A., Rasmussen, F.O., Siemers, T., Søiland, G. & Tirsgaard, H. (Fritsen, A. ed.) 1996: Description and Classification of Chalks North Sea Central Graben. Joint Chalk Research Phase IV.
Cronan, D.S. 1974: Authigenic minerals in deep-sea sediments. In: Goldberg, E.D. (ed): The Sea, 5, John Wiley & Sons, New York, 491- 525.
Damholt, T. & Surlyk, F. 2004: Laminated-bioturbated cycles in Maastrichtian chalk of the North Sea: oxygenation fluctuations within the Milankovitch frequency band. Sedimentology 51, 1323–1342.
Delage, P., Cui, Y.J., Schroeder, C. 1996: Subsidence and capillary effects in chalks. Eurock '96, ISRM International Symposium, Torino, Italy, 1291– 1298.
Delaney, M.L. & Linn, L.J. 1993: Interstitial water and bulk calcite chemistry, Leg 130, and calcite recrystallization. Proceedings of the Ocean Drilling Program Scientific Results 130, 561-572.
Dewers, T. & Ortoleva, P. 1990: Force of crystallization during the growth of siliceous concretions. Geology 18, 204-207.
D'Hondt, S.L., Jørgensen, B.B., Miller, D.J., *et al*. 2003: Proc. ODP, Init. Repts., 201: College Station, TX (Ocean Drilling Program). doi:10.2973/odp.proc.ir.201.2003
Doyle, C. & Conlin, J.M. 1990: The Tyra Field. In: Buller, A.T., Berg, E. *et al.* (eds): North Sea Oil and Gas Reservoirs–II, 47-65, The Norwegian Institute of Technology, Graham & Trotman.
Dvorkin, J., Nur, A. & Yin, H. 1994: Effective properties of cemented granular materials: Mechanics of Materials 18, 351-366.
Ekdale, A.A. & Bromley, R.G. 1984: Comparative ichnology of shelf-sea and deep-sea chalk. Journal of Paleontology 58, 322-332.
Engstrøm, F. 1995: A new method to normalize capillary pressure curves. Paper 9535 presented at the International Symposium of the Society of Core Analysts, California, USA, 12 pp.
Fabricius, I.L. 2000: Interpretation of burial history and rebound from loading experiments and the occurrence of microstylolites in the mixed sediments of the Caribbean Sites 999 and 1001: Proceedings of the Ocean Drilling Program, Scientific Results 165, 177-190.
Fabricius, I.L. 2001: Compaction of microfossil and clay-rich chalk sediments. Physics and Chemistry of the Earth 26, 59-62.
Fabricius, I.L. 2003: How burial diagenesis of chalk sediments controls sonic velocity and porosity. American Association of Petroleum Geologists Bulletin 87, 1755-1778.
Fabricius, I.L. & Borre, M.K. 2007: Stylolites, porosity, depositional texture, and silicates in chalk facies sediments. Ontong Java Plateau – Gorm and Tyra fields, North Sea. Sedimentology 54, 183-205.
Fabricius, I.L. & Shogenova, A. 1998: Acoustic velocity data for clay bearing carbonate rocks from the Paleozoic deposits of Estonia and the Cenozoic and Mesozoic deposits of the Caribbean Sea. In: Middleton, M.F. (ed.): Nordic Petroleum Series IV: Research in Petroleum Technology, 111-123.
Fabricius, I.L., Olsen, C. & Prasad, M. 2005: Log interpretation of marly chalk, the Lower Cretaceous Valdemar Field, Dan-

ish North Sea: Application of iso-frame and pseudo water film concepts. The Leading Edge 24, 496-505.
Fabricius, I.L., Høier, C., Japsen, P. & Korsbech, U. 2007a: Modeling elastic properties of impure chalk from the South Arne Field, North Sea. Geophysical Prospecting 55, 487-506.
Fabricius, I.L., Røgen, B. & Gommesen, L. 2007b: How depositional texture and diagenesis control petrophysical and elastic properties of samples from five North Sea chalk fields. Petroleum Geoscience 13, 81-95.
Fabricius, I.L., Gommesen, L., Krogsbøll, A. & Olsen, D. in press: Terzaghi's law and Biot's coefficient for interpretation of porosity- and velocity- depth trends in chalk – effect of admixtures of clay minerals and quartz. American Association of Petroleum Geologists Bulletin.
Farmer, C.L. & Barkved, O.I. 1999: Influence of syn-depositional faulting on thickness variations in chalk reservoirs – Valhall and Hod fields. In: Fleet, A.J. & Boldy, S.A.R. (eds): Petroleum Geology of Northwest Europe: Proceedings of the 5th Conference. Petroleum Geology´86 Ltd. Geological Society, London, 949-957.
Farrell J.W. & Prell W.L. 1989: Climatic change and CaCO3 preservation: An 800,000 year bathymetric reconstruction from the central equatorial Pacific Ocean. Paleoceanography 4, 447-466
Fjær, E., Holt, R. M., Horsrud, P., Raaen, A.M. & Risnes, R. 1992: Petroleum related rock mechanics, Developments in Petroleum Science 33, Elsevier.
Frykman, P. & Deutsch, C.V. 2002: Practical Application of Geostatistical Scaling Laws for Data Integration. Petrophysics, 43, 153-171.
Gassmann, F. 1951: Elastic waves through a packing of spheres. Geophysics 16, 673-685.
Gommesen, L. & Fabricius, I.L. 2001: Dynamic and Static Elastic Moduli of North Sea and Deep Sea Chalk. Physics and Chemistry of the Earth 26, 63-68.
Gommesen, L., Fabricius, I.L., Mukerji, T., Mavko, G. & Pedersen, J.M. 2007: Elastic behaviour of North Sea chalk: A well log study. Geophysical Prospecting 55, 307-322.
Håkansson, E., Bromley, R., and Perch-Nielsen, K. 1974: Maastrichtian chalk of northwest Europe–a pelagic shelf sediment. In K. J. Hsü and H. C. Jenkyns eds. Pelagic Sediments on Land and Under the Sea. Special Publication of the International Association of Sedimentologists 1, 211-233.
Hancock, J.M. 1975: The petrology of the chalk. Proc. Geol. Assoc., 86, 499–535.
Harstad, A.O. & Stipp, S.L.S. 2007: Calcite dissolution: Effects of trace cations naturally present in Iceland spar calcites. Geochimica et Cosmochimica Acta 71, 56–70.
Hashin, Z. & Shtrikman, S. 1963: A variational approach to the elastic behavior of multiphase materials. Journal of the Mechanics and Physics of Solids 11, 127-140.
Hatton, I.R. 1986: Geometry of allochtonous Chalk Group members, Central Trough, North Sea. Marine and Petroleum Geology 3, 79-98.
Heggheim, T., Madland, M.V., Risnes, R. & Austad, T. 2005: A chemical induced enhanced weakening of chalk by seawater. Journal of Petroleum Science and Engineering 46, 171– 184.
Hellmann, R., Renders, P.J.N., Gratier, J.-P. & Guiguet, R. 2002: Experimental pressure solution compaction of chalk in aqueous solutions: Part 1. Deformation behaviour and chemistry. In: Hellmann, R. & Wood, S.C. (eds.): Water–rock Interactions, Ore Deposits, and Environmental Geochemistry: A tribute to David A. Crerar, The Geochemical Society, Special Publication 7, 129-152.
Henriksen A., Fabricius, I.L., Borre, M.K., Korsbech, U., Theilgaard, A.T. & Zandbergen, J.B. 1999: Core density scanning and mechanical properties of limestone in the Copenhagen area. Quarterly Journal of Engineering Geology 32, 107-117.
Henriksen, K., Stipp, S.L.S., Young, J.R. & Marsh, M.E. 2004: Biological control on calcite crystallization: AFM investigation of coccolith polysaccharide Function. American Mineralogist 89, 1709-1716.
Herrington, P.M., Pederstad K., & Dickson, J.A.D. 1991: Sedimentology and Diagenesis of Resedimented and Rhythmically Bedded Chalks from the Eldfisk Field, North Sea Central Graben. American Association of Petroleum Geologists Bulletin 75, 1661 – 1674.
Hill, P.R. 1983: Chalk solution structures in cores from Deep Sea Drilling Project Leg 94. Initial reports of the Deep Sea Drilling Project 94, 1129-1143.
Hurst, C. 1983: Petroleum geology of the Gorm field, Danish North Sea. Geol. Mijnbouw 62, 157-168.
Hvid, J.M., 1998: Influence of depositional texture and porosity on ultrasonic wave propagation in Danian limestone from eastern Denmark. In: Middleton, M.F. (ed.): Research in petroleum technology: Gøteborg, Vasastadens Bokbinderi AB, Nordic Petroleum Series IV, ISBN 82-994330-3-7, 125-154.
Jacobsen, N.L., Engstrøm, F., Uldall, A. & Petersen, N.W. 1999: Delineation of hydrodynamic/geodynamic trapped oil in low permeabiliy chalk, SPE 56514, 10 pp.
Jakobsen, F., Ineson, J.R., Kristensen, L. & Stemmerik, L. 2004: Characterization and zonation of a marly chalk reservoir: the Lower Cretaceous Valdemar Field of the Danish Central Graben. Petroleum Geoscience 10, 21-33.
Japsen, P. 1998: Regional velocity-depth anomalies, North Sea chalk: a record of overpressure and Neogene uplift and erosion. American Association of Petroleum Geologists Bulletin 82, 2031-2074.
Japsen, P., Bruun, A., Fabricius, I.L., Rasmussen, R., Vejbæk, O.V., Pedersen, J.M., Mavko, G., Mogensen, C. & Høier, C. 2004: Influence of porosity and pore fluid on acoustic properties of chalk: AVO response from oil, South Arne Field, North Sea. Petroleum Geoscience 10, 319-330.
Jørgensen, N.O. 1987: Oxygen and carbon isotope composition of Upper Cretaceous chalk from Danish sub-basin and the North Sea Central Graben. Sedimentology, 34, 559-570.
Jones, M.E., Bedford, J. & Clayton, C.J. 1984: On natural deformation mechanisms in the chalk. Journal of Geological Society (London) 141, 675-683.
Kastner, M. 1981: Authigenic silicates in deep-sea sediments: formation and diagenesis. In: Emiliani, C. (ed.): The Oceanic Lithosphere, Sea 7, 915-980. John Wiley & Sons, New York.
Kennedy, W.J. & Garrison, R.E. 1975: Morphology and genesis of nodular chalks and hardgrounds in the Upper Cretaceous of southern England. Sedimentology 22, 311-86.
Kozeny, J. 1927: Über kapillare leitung des Wassers im Boden. Sitzungsberichte der Wiener Akademie des Wissenschaften 136, 271-306.
Kristensen, L., Dons, T., Maver, K.G. & Schiøler, P. 1995: A multidisciplinary approach to reservoir subdivision of the Maastrichtian chalk in the Dan field, Danish North Sea. American Association of Petroleum Geologists Bulletin 79, 1650-1660.

Kroenke, L.W., Berger, W.H., Janecek, T.R. *et al.* 1991: Proc. ODP Init. Repts., 130, 1-1240. College Station, TX (Ocean Drilling Program).

Krogsbøll, A. & Foged, N. 2003: Effects of simultaneous consolidation and creep on interpretation of test results. In Di Benedetto et al. eds. Deformation Characteristics of Geomaterials, Proceedings of the third Int. Symp. Deformation characteristics of Geomaterials, IS LYON 2003, Lyon, France. Balkema, Lisse, 6pp.

Larsen, J.K. & Fabricius, I.L. 2004: Interpretation of water saturation above the transitional zone in chalk reservoirs. SPE Reservoir Evaluation & Engineering 7, 155-163.

Lawrence, J.R. & Gieskes, J.M. 1981: Constraints on water transport and alteration in the oceanic crust from the isotopic composition of pore water. Journal of Geophysical Research 86, 7924-7934.

Lind, I. 1991: Microprobe aided mapping of areal element concentration and microporosity in chalk. Carbonates and Evaporites 6, 45-51.

Lind, I.L. 1993a: Stylolites in chalk from Leg 130, Ontong Java Plateau. Proceedings of the Ocean Drilling Program Scientific Results 130, 445-451.

Lind, I.L. 1993b: Loading experiments on carbonate ooze and chalk from Leg 130, Ontong Java Plateau. Proceedings of the Ocean Drilling Program Scientific Results 130, 673-686.

Lind, I. 1997: A modified Wyllie equation for the relationship between porosity and sonic velocity of mixed sediments and carbonates from the Caribbean Sea. In: Middleton, M. F. ed. Nordic Petroleum Series III: Research in Petroleum Technology. 123-137.

Lind, I. & Grøn, P. 1996: Porosity variation in chalk. Zentralblatt für Geoleologie und Paläontologie Teil 1 1994, 1447-1457.

Lind, I. & Schiøler, P. 1994: Dinoflagellate cyst concentration as an independent reference for monitoring mineral mobilization in stylolites. Sedimentary Geology 92, 53-65.

Lind, I.L., Janecek, T., Krissek, L., Prentice, M., & Stax, R. 1993: Color bands in Ontong Java Plateau carbonate oozes and chalks. Proc. ODP Sci. Results, 130, 453-470.

Lind, I., Nykjær, O., Priisholm, S. & Springer, N. 1994: Permeability of stylolite-bearing chalk. Journal of Petroleum Technology 46, 986-993.

Lindgreen, H., Drits, V.A., Sakharov, B.A., Jakobsen, H.J., Salyn, A.L., Dainyak, L.G. & Krøyer, H. 2002: The structure and diagenetic transformation of illite-smectite and chlorite-smectite from North Sea Cretaceous-Tertiary chalk: Clay Minerals 37 429-450.

Lyons, T.W., Murray, R.W. & Pearson, D.G. 2000: Highlights from pore-water results.: Diagenetic pathways in sediments of the Caribbean Sea. Proceedings of the Ocean Drilling Program, Scientific Results 165, 287-298.

Mackertich, D.S. & Goulding, D.R.G. 1999: Exploration and appraisal of the South Arne Field, Danish North Sea. In: Fleet, A.J. & Boldy, S.A.R. (eds): Petroleum Geology of Northwest Europe: Proceedings of the 5th Conference. Petroleum Geology´86 Ltd. Geological Society, London, 959-974.

Madirazza, I. 1965: Structural geology of a limestone mine at Mønsted, Northern Jutland. Bull. Geol. Soc. Denmark 15, 519-547.

Madsen, L. & Lind, I. 1998: Adsorption of carboxylic acids on reservoir minerals from organic and aqueous phase. SPE Reservoir Evaluation and Engineering 1, 47-51.

Madsen, L., Grahl-Madsen, L., Grøn, C., Lind, I. & Engell, J. 1996: Adsorption of polar aromatic hydrocarbons on synthetic calcite. Organic Geochemistry 24, 1151-1155.

Madsen, L., Grøn, C., Lind, I. & Engell, J. 1998: Adsorption of benzoic acid on synthetic calcite dispersed in cyclohexane as a function of temperature. Journal of Colloid and Interface Science 205, 53-64.

Maliva, R.G. & Dickson, J.A.D. 1992: Microfacies and diagenetic controls of porosity in Cretaceous/Tertiary chalks, Eldfisk Field, Norwegian North Sea. American Association of Petroleum Geologists Bulletin 76, 1825-1838.

Maliva, R.G. & Siever, R. 1989: Nodular chert formation in carbonate rocks. Journal of Geology 97, 421-433.

Mavko G., Mukerji, T. & Dvorkin, J. 1998: The Rock Physics Handbook: Cambridge University Press.

Megson, J.B. 1992: The North Sea chalk play; examples from the Danish Central Graben. In: Hardman, R.F.P. (ed.): Exploration Britain: Geological insights for the next decade. Geological Society Special Publication (London) 67, 247--282.

Mortensen, J., Engstrøm, F. & Lind, I., 1998: The relation among porosity, permeability, and specific surface of chalk from the Gorm field, Danish North Sea. SPE 31062, SPE Reservoir Evaluation & Engineering 1, 245-251.

Musgrave, R.J., Delaney, M.L., Stax, R. & Tarduno, J.A., 1993: Magnetic diagenesis, organic input, interstitial water chemistry, and paleomagnetic record of the carbonate sequence of the Ontong Java Plateau. Proceedings of the Ocean Drilling Program Scientific Results 130, 527-546.

Mutti, M. 2000: Bulk $\delta^{18}O$ and $\delta^{13}C$ records from Site 999, Columbian Basin, and Site 1000, Nicaragua Rise (latest Oligocene to Middle Miocene): diagenesis, link to sediment parameters, and paleoceanography. Proceedings of the Ocean Drilling Program, Scientific Results 165, 275-283.

Mutti, M. & Bernoulli, D. 2003: Early marine lithification and hardground development on a Miocene ramp (Maiella, Italy): Key surfaces to track changes in trophic resources in nontropical carbonate settings. Journal of Sedimentary Research 73, 296-308.

Neugebauer, J. 1974: Some aspects of cementation in chalk. In: Hsü, K.J. & Jenkyns, H.J. (eds): Pelagic Sediments on Land and Under the Sea. Special Publication of the International Association of Sedimentologists 1, 149-176.

Nur, A. & Byerlee, J.D. 1971: An exact effective stress law for elastic deformation of rocks with fluids. Journal of Geophysical Research 76, 6414-6419.

Olsen, C., Christensen, H.F. & Fabricius, I.L. in press a: Static and dynamic Young's modulus of chalk from the North Sea. Geophysics.

Olsen, C., Hedegaard, K., Fabricius, I.L. & Prasad, M. in press b: Prediction of Biot's coefficient from rock physical modeling of North Sea chalk. Geophysics.

Perch-Nielsen, K. 1979: Calcareous nannofossil zonation at the Cretaceous/Tertiary boundary in Denmark. In: Birkelund, T. & Bromley, R.G. (eds): Cretaceous-Tertiary Boundary Events Symposium. University of Copenhagen, Copenhagen, 115-135.

Prasad, M., Fabricius, I.L. & Olsen, C. 2005: Rock physics and statistical well log analysis in marly chalk. The Leading Edge 25, 491-495.

Risnes, R. 2001: Deformation and Yield in High Porosity Outcrop Chalk. Phys. Chem. Earth (A), 26, 53-57.

Risnes, R., Madland, M.V., Hole, M. & Kwabiah, N.K. 2005: Water weakening of chalk— Mechanical effects of water–

glycol mixtures. Journal of Petroleum Science and Engineering 48, 21– 36.
Røgen, B. & Fabricius, I.L. 2002: Influence of clay and silica on permeability and capillary entry pressure of chalk reservoirs in the North Sea. Petroleum Geoscience 8, 287-293.
Røgen, B., Gommesen, L. & Fabricius, I.L. 2001: Grain size distributions of chalk from image analysis of electron micrographs. Computers and Geoscience 27, 1071-1080.
Røgen, B., Gommesen, L. & Fabricius, I.L. 2004: Methods of velocity prediction tested for North Sea chalk: a review of fluid substitution and $v_S$ estimates. Journal of Petroleum Science and Engineering 45, 129-139.
Røgen, B., Fabricius, I.L., Japsen, P., Høier, C., Mavko, G. & Pedersen, J.M. 2005: Ultrasonic velocities of North Sea chalk samples: influence of porosity, fluid content and texture. Geophysical Prospecting 53, 481-496.
Ruddy, I., Andersen, M.A., Pattillo, P.D., Bishlawi, M. & Foged, N. 1989: Rock compressibility, compaction, and subsidence in a high-porosity chalk reservoir: a case study of Valhall field. Journal of Petroleum Technology 41, 741-746.
Safaricz, M. & Davison, I. 2005: Pressure solution in chalk. AAPG Bulletin 89, 383-401.
Scholle, P. A. 1977: Chalk diagenesis and its relation to petroleum exploration: oil from chalks, a modern miracle? American Association of Petroleum Geologists Bulletin 61, 982-1009.
Scholle, P.A., Albrechtsen, T. & Tirsgaard, H. 1998: Formation and diagenesis of bedding cycles in uppermost Cretaceous chalks of the Dan Field, Danish North Sea. Sedimentology 45, 223-243.
Schön, J.H. 1996: Physical properties of rocks: fundamentals and principles of petrophysics. Helbig, K. & Treitel, S. eds. Handbook of Geophysical Exploration, Seismic Exploration 18, 583 pp.
Sigurdsson, H., Leckie, R.M., Acton, G.D. *et al.* 1997: Proc. ODP Init. Repts., 165, 1-862. College Station, TX (Ocean Drilling Program).
Simonsen, L. & Toft, J. 2006: Texture, composition and stratigraphy of volcanic ash beds in lower Paleocene chalk from the North Sea Central Graben. Marine and Petroleum Geology 23, 767-776.
Stax, R. & Stein R. 1993: Long-term changes in the accumulation of organic carbon in Neogene sediments , Ontong Java Plateau. Proceedings of the Ocean Drilling Program Scientific Results 130, 573-584.
Stipp, S.L.S. 2002: Where the bulk terminates: experimental evidence for restructuring, chemibond OH- and H+, adsorbed water and hydrocarbons on calcite surfaces. Molecullar Simulation 28, 497-516.
Surlyk, F. 1997: A cool-water carbonate ramp with bryozoan mounds: Late Cretaceous–Danian of the Danish basin. In: James, N.P. & Clarke, J.D.A. (eds): Cool-water carbonates: SEPM (Society for Sedimentary Geology) Special Publication 56, 293–308.
Terzaghi, K. 1923: Die Berechnung der Durcglässigkeitsziffer des Tones aus dem Verlauf der hydrodynamischen Spannungserscheinungen. Sitzungsber. Akad. Wiss. Wien. Math. Naturwiss. K., Abt. 2A 132 125-132 138.
Urmos, J. & Wilkens, R.H. 1993: In situ velocities in pelagic carbonates: New insights from ocean drilling program leg 130, Ontong Java. Journal of Geophysical Research 98, B5, 7903-7920.
Urmos, J., Wilkens, R.H., Bassinot, F., Lyle, M, Masters, J.C., Mayer, L.A. & Mosher, D. 1993: Laboratory and well-log velocity and density measurements from the Ontong Java Plateau: new in-situ corrections to laboratory data for pelagic carbonates. Proceedings of the Ocean Drilling Program Scientific Results 130, 607-622.
Vejbæk, O.V., Rasmussen, R., Japsen, P., Bruun, A., Pedersen, J.M., Marsden, G., & Fabricius, I.L. 2005: Modeling seismic response from North Sea chalk reservoirs resulting from changes in burial depth and fluid saturation. In: Doré, A.G. & Vinning, B.A. (eds): Petroleum Geology: North-West Europe and Global Perspectives –Proceedings of the 6th Petroleum Geology Conference, 1401-1413. Petroleum Geology Conferences Ltd., Geological Society, London.
Walls, J.D., Dvorkin, J. & Smith, B.A. 1998: Modeling seismic velocity in Ekofisk Chalk. 68th SEG Meeting, New Orleans, U.S.A. Expanded abstracts, 1016-1019.
Wanless, H.R. 1979: Limestone response to stress: pressure solution and dolomitization. Journal of Sedimentary Petrology 49, 437-462.
Waples, D.W. 1980: Time and temperature in petroleum formation: Application of Lopain's method to petroleum exploration. American Association of Petroleum Geologists Bulletin 64, 916-926.
Warpinsky, N.R. & Teufel, L.W. 1992: Determination of the effective stress law for permeability and deformation in low-permeability rocks. SPE Formation Evaluation 7, 123-131.
Williams, L.A., Parks, G.A. & Crerar, D.A. 1985: Silica diagenesis, I. Solubility controls. Journal of Sedimentary Petrology 55, 301-311.
Williams, L.A. & Crerar, D.A. 1985: Silica diagenesis, II. General mechanisms. Journal of Sedimentary Petrology 55, 312-321.
Zubtsov, S., Renard, F., Gratier, J.-P., Dysthe, D.K. & Trakine, V. 2005: Single-contact pressure solution creep on calcite monocrystals. In: Gapais, D., Brun, J.P. & Cobbold, P.R. (eds): Deformation Mechanisms, Rheology and Tectonics: from Minerals to the Lithosphere: Geological Society, London, Special Publications 243, 81-95.